

Imprints of local lightcone projection effects on the galaxy bispectrum. II

Sheean Jolicoeur^a, Obinna Umeh^a, Roy Maartens^{a,b} and Chris Clarkson^{a,c,d}

^a*Department of Physics & Astronomy, University of the Western Cape, Cape Town 7535, South Africa*

^b*Institute of Cosmology & Gravitation, University of Portsmouth, Portsmouth PO1 3FX, United Kingdom*

^c*School of Physics & Astronomy, Queen Mary University of London, London E1 4NS, United Kingdom*

^d*Department of Mathematics & Applied Mathematics, University of Cape Town, Cape Town 7701, South Africa*

(Dated: October 2, 2017)

General relativistic imprints on the galaxy bispectrum arise from observational (or projection) effects. The lightcone projection effects include local contributions from Doppler and gravitational potential terms, as well as lensing and other integrated contributions. We recently presented for the first time, the correction to the galaxy bispectrum from all local lightcone projection effects up to second order in perturbations. Here we provide the details underlying this correction, together with further results and illustrations. For moderately squeezed shapes, the correction to the Newtonian prediction is $\sim 30\%$ on equality scales at $z \sim 1$. We generalise our recent results to include the contribution, up to second order, of magnification bias (which affects some of the local terms) and evolution bias.

CONTENTS

I. Introduction	2
II. Galaxy number counts in general relativity	4
II.1. Local model of galaxy bias on ultra-large scales	5
II.2. Observed galaxy number counts in Poisson gauge	7
III. Galaxy number overdensity in Fourier space and the bispectrum	10
IV. Numerical Results	13
V. Conclusion	17
A. Second-order gauge transformation of number density contrast	18
B. Expansion of perturbed variables in Fourier space	19
C. The coefficients in the GR kernel $\mathcal{K}_{\text{GR}}^{(2)}$	22
References	24

I. INTRODUCTION

The galaxy power spectrum has been central to the cosmological constraints extracted from galaxy surveys up to now. For an accurate comparison of observations to theory, observational projection effects on the galaxy power spectrum must be taken into account. The main projection effect comes from redshift-space distortions (RSD) [1–3], which must be included in the analysis of the power spectrum. But it is not only accuracy that is gained – there is additional information to be extracted from the RSD themselves.

In addition to RSD, the galaxy power spectrum is also affected by lensing magnification [4–6]. In the analysis of current surveys, the lensing contribution to galaxy number counts is typically not included in the power spectrum. For future surveys, which will probe higher redshifts, this lensing projection effect will need to be included in the galaxy power spectrum for an accurate theoretical analysis – and, as with RSD, the lensing itself will deliver additional information [7–9].

Lensing convergence contributes a general relativistic (GR) projection effect, which is a correction to the Newtonian (overdensity + RSD) galaxy power spectrum. There are further GR projection effects which modify the galaxy power spectrum on ultra-large scales ($H_0 \lesssim k \lesssim k_{\text{eq}}$) [10–12]. These include Doppler, Sachs-Wolfe, integrated Sachs-Wolfe and time-delay terms. As in the case of RSD and lensing, these terms need to be incorporated for accuracy, and they also contain extra information.

The ultra-large scale GR corrections have a qualitatively similar effect on the galaxy power spectrum to primordial non-Gaussianity (PNG), which also modifies the power spectrum on ultra-large scales via scale-dependent galaxy bias. The GR corrections must therefore be taken into account when super-equality scales are probed to measure or constrain the PNG parameter f_{NL} [13–17].

The galaxy bispectrum can provide additional information, partly independent of the power spectrum [18, 19]. The effects on the bispectrum from RSD have been computed in [20, 21] and from lensing in [22]. Recently, the galaxy bispectrum has been used to detect the RSD and baryon acoustic oscillation (BAO) features in the BOSS survey, and to give independent measurements of growth rates and distances [23, 24].

As in the case of the galaxy power spectrum, we need to take account of the observational lightcone effects in the galaxy bispectrum which distort the information on the underlying dark matter distribution, but which also provide new information. These projection effects are the same as for the power spectrum – with one major difference: for the bispectrum, we require the projection effects up to at least second order in perturbations.

Next-generation galaxy surveys will enable increasingly accurate measurements of the galaxy bispectrum, out to higher redshifts and across larger sky areas. Recent forecasts, using a Newtonian model with RSD but no GR projection effects, indicate that the bispectrum can considerably enhance the constraining power of future surveys [25] – especially for probing the initial conditions of the Universe via PNG. In order to fully exploit the improved precision from upcoming surveys, we need theoretical accuracy that matches and moves beyond observational precision. One important part of this theoretical requirement is to include all the GR projection effects in modelling the galaxy bispectrum.

The GR lightcone effects on the galaxy angular bispectrum from lensing convergence were computed on intermediate scales in [26], neglecting the other, ultra-large scale, GR corrections to the galaxy overdensity. Another partial result was given in [27], using a separate-universe approximation to compute the galaxy angular bispectrum with all GR lightcone effects in the squeezed limit.

We recently provided a further partial result, valid for all triangle shapes, by computing all the local GR projection corrections to the galaxy bispectrum, including all second order terms and couplings [28]. Crucial to our result is the expression for the observed galaxy number counts on the past lightcone, up to second order. This is given in the most general case by [29] (see also [30–33]). Our work is complementary to the subsequent work by [34], who include lensing and terms of order $(\mathcal{H}/k)[\delta^{(1)}]^2$, but neglect all other GR effects on ultra-large scales.

Here we provide details of the derivation of the results given in [28], with additional illustrations, and we generalise some of those results. In particular, we include the magnification bias (which also contributes to local terms in the number counts) and the evolution bias. In [28], both of these were set to zero.

We focus on large enough scales that perturbation theory is accurate, and we make the following assumptions:

- A Gaussian primordial curvature perturbation.
- A simple local-in-mass-density model of galaxy bias, as in [18, 19] (schematically, $\delta_g \sim b_1 \delta_m + b_2 \delta_m^2/2$). However, we take care to ensure that the definition of bias is gauge-independent and applies on ultra-large scales.
- For simplicity, we use standard Newtonian results to evaluate the second-order velocity potential $v^{(2)}$ and metric potentials $\Phi^{(2)}, \Psi^{(2)}$, which contribute to the projection effects.
- We neglect the second-order effect of the radiation era on initial conditions for sub-equality modes [35].

- We compute the galaxy bispectrum at fixed redshift and in Fourier space, and we use the plane-parallel approximation. Consequently, the following are not included in our approach: wide-angle correlations, radial correlations, lensing and other integrated contributions.

At second order in GR, scalar perturbations generate secondary vector and tensor modes [36, 37]. These modes also enter the projection effects in the observed galaxy number density contrast at second order [29–33]. As shown by [38, 39] for vector modes and [40–42] for tensor modes, the power in the secondary vector and tensor modes is much smaller than the scalar power at second order, so we neglect the vector and tensor contributions.

We adopt a standard concordance model, with parameters given by the latest Planck best-fit values [43]; in particular, $h = H_0/(100 \text{ km s}^{-1} \text{ Mpc}^{-1}) = 0.678$ and $\Omega_{m0} = 1 - \Omega_{\Lambda0} = 0.308$.

II. GALAXY NUMBER COUNTS IN GENERAL RELATIVITY

The observer looks down the past lightcone and counts dN galaxies, above a threshold luminosity L , within a redshift interval dz about the observed redshift z , and within a solid angle element $d\Omega_o$ about the observed direction \mathbf{n} , where [7, 11, 15, 29]

$$dN(z, \mathbf{n}, > \ln L) = \mathcal{N}(z, \mathbf{n}, > \ln L) D_A^2(z, \mathbf{n}) k_\mu u^\mu \frac{d\lambda}{dz} dz d\Omega_o. \quad (1)$$

Here D_A is the angular diameter distance, u^μ is the 4-velocity of the source, $k^\mu = dx^\mu/d\lambda$ is the geodesic photon 4-momentum, and \mathcal{N} is the flux-limited number density of sources:

$$\mathcal{N}(z, \mathbf{n}, > \ln L) = \int_{\ln L}^{\infty} d \ln \tilde{L} n_g(z, \mathbf{n}, \ln \tilde{L}). \quad (2)$$

In the integrand, n_g is the proper number density of sources, and only sources with luminosity above the detection threshold are counted by the observer.

The fractional perturbation Δ_g of the observed number counts is defined by

$$\frac{dN(z, \mathbf{n}, > \ln L)}{dz d\Omega_o} = \frac{\chi^2(z)}{(1+z)^4 \mathcal{H}(z)} \bar{\mathcal{N}}(z, > \ln L) [1 + \Delta_g(z, \mathbf{n}, > \ln L)], \quad (3)$$

where $\mathcal{H}(\eta) = a'(\eta)/a(\eta)$ is the conformal Hubble rate, the comoving line-of-sight distance is given by $d\chi = dz/[(1+z)\mathcal{H}(z)]$, and $\bar{\mathcal{N}}$ is the background magnitude-limited number density. Henceforth, we suppress the dependence of Δ_g on $\ln L$ to reduce clutter. We expand Δ_g up to second order in perturbation theory:

$$\Delta_g(z, \mathbf{n}) = \Delta_g^{(1)}(z, \mathbf{n}) + \frac{1}{2} \left[\Delta_g^{(2)}(z, \mathbf{n}) - \langle \Delta_g^{(2)}(z, \mathbf{n}) \rangle \right], \quad (4)$$

where we subtract off the average of $\Delta_g^{(2)}$ in order to ensure that $\langle \Delta_g \rangle = 0$. For later convenience, we split the observed number density contrast into Newtonian and GR parts:

$$\Delta_g^{(r)} = \Delta_{gN}^{(r)} + \Delta_{gGR}^{(r)}, \quad r = 1, 2. \quad (5)$$

We only consider the bispectrum at fixed redshift, so that all correlations are in the same redshift bin. There are integrated GR contributions to $\Delta_g^{(1)}$, from weak lensing convergence and also from integrated Sachs-Wolfe and time-delay terms, and we neglect these terms. At second order, there are many more terms with line-of-sight integrated contributions, and we neglect all such terms. Specifically, we neglect the integrated contributions in [29], which gives the fully general $\Delta_g^{(1)}$ and $\Delta_g^{(2)}$ in Poisson gauge.¹ A complete treatment would include the integrated terms, with all cross-bin correlations. This far more complicated analysis is left for future work.

An important point to note is that the GR weak lensing convergence consists not only of the standard integrated term, but also includes local (non-integrated) terms [44]. This means that the magnification bias will still enter the bispectrum, even if we neglect all integrated terms. The magnification bias is given by the logarithmic slope of the background number density at the threshold luminosity:

$$\mathcal{Q}(a, \bar{L}) = - \frac{\partial \ln [a^3 \bar{\mathcal{N}}(a, > \bar{L})]}{\partial \ln \bar{L}}. \quad (6)$$

We have used the comoving number density in the definition above since it arises also in the definition of the evolution bias:

$$b_e(a, \bar{L}) = \frac{\partial \ln [a^3 \bar{\mathcal{N}}(a, > \bar{L})]}{\partial \ln a}. \quad (7)$$

This quantity describes the deviation of the background number density of sources from the idealised case of $a^3 \bar{\mathcal{N}} = \bar{\mathcal{N}}_0$.

Radial and transverse derivatives are defined as

$$\partial_{\parallel} = n^i \partial_i, \quad \partial_{\perp i} = \partial_i - n_i \partial_{\parallel}, \quad (8)$$

¹ We also neglect all terms at the observer, which do not contribute to the bispectrum.

the derivative down rays of the past lightcone is

$$\frac{d}{d\chi} = -\frac{d}{d\eta} = -\partial_\eta + \partial_\parallel, \quad (9)$$

and the screen space projected Laplacian is

$$\nabla_\perp^2 = \nabla^2 - \partial_\parallel^2 - \frac{2}{\chi}\partial_\parallel. \quad (10)$$

Since Δ_g is defined as an observable, it is gauge-independent and we can use any gauge to compute it. In a given gauge, it will be of the form $\Delta_g = \delta_g +$ terms that describe projection effects in that gauge, where $\delta_g = \delta\mathcal{N}/\mathcal{N} = \delta_g^{(1)} + \frac{1}{2}\delta_g^{(2)}$ is the galaxy number density contrast in the chosen gauge. We choose the Poisson gauge since it is convenient for splitting into Newtonian and GR parts. Neglecting the vector and tensor modes, the metric and the peculiar velocity of galaxies (equal to the dark matter velocity on the scales of interest) are given by

$$a^{-2}ds^2 = -\left[1 + 2\Phi^{(1)} + \Phi^{(2)}\right]d\eta^2 + \left[1 - 2\Phi^{(1)} - \Psi^{(2)}\right]d\mathbf{x}^2, \quad (11)$$

$$v^i = \partial^i\left[v^{(1)} + \frac{1}{2}v^{(2)}\right]. \quad (12)$$

The observed comoving coordinates [30] of a galaxy are $\mathbf{x} = \chi(z)\mathbf{n} = [\eta_0 - \eta(z)]\mathbf{n}$. We have assumed that anisotropic stress vanishes at first order, which implies $\Psi^{(1)} = \Phi^{(1)}$ in GR.

We will also use the comoving-synchronous (C) overdensities of matter and galaxy counts δ_{mC}, δ_{gC} . The first-order Poisson and continuity equations are then

$$\nabla^2\Phi^{(1)} = \frac{3}{2}\Omega_m\mathcal{H}^2\delta_{mC}^{(1)}, \quad \delta_{mC}^{(1)'} = -\nabla^2v^{(1)}, \quad (13)$$

which lead to

$$\Phi^{(1)} = -\frac{3}{2}\Omega_m\frac{\mathcal{H}^2}{k^2}\delta_{mC}^{(1)} \quad \text{where} \quad \Phi^{(1)}(a, \mathbf{k}) = \frac{D(a)}{a}\Phi^{(1)}(1, \mathbf{k}), \quad (14)$$

$$\mathcal{H}v^{(1)} = f\frac{\mathcal{H}^2}{k^2}\delta_{mC}^{(1)} \quad \text{where} \quad f = \frac{d\ln D}{d\ln a} \quad \text{and} \quad \delta_{mC}^{(1)}(a, \mathbf{k}) = D(a)\delta_{mC}^{(1)}(1, \mathbf{k}). \quad (15)$$

II.1. Local model of galaxy bias on ultra-large scales

We start by considering the Poisson-gauge number density contrast $\delta_g^{(1)}$ at linear order, which is related to the dark matter density contrast $\delta_m^{(1)}$ via the galaxy bias. We need to ensure that the definition of scale-independent galaxy bias is gauge-independent and valid on ultra-large scales. As explained in detail in [11, 13, 15], the physical definition of scale-independent bias is in the matter rest-frame, which coincides with the galaxy rest-frame (on large scales there is no velocity bias). The matter rest-frame corresponds to the C gauge, so that the correct definition at first order is (restoring the dependence on L):

$$\delta_{gC}^{(1)}(a, \mathbf{x}, < \ln L) = b_1(a, \ln \bar{L})\delta_{mC}^{(1)}(a, \mathbf{x}). \quad (16)$$

The Poisson-gauge number density contrast is related to the C-gauge one by [11]

$$\delta_g^{(1)} = \delta_{gC}^{(1)} + (3 - b_e)\mathcal{H}v^{(1)} = b_1\delta_{mC}^{(1)} + (3 - b_e)\mathcal{H}v^{(1)}. \quad (17)$$

The velocity potential term in (17) ensures gauge-independence of the bias model on ultra-large scales. This term is the GR part of $\delta_g^{(1)}$, since it is suppressed on small scales but grows on ultra-large scales, as shown by (15).

In GR, the Lagrangian frame corresponds to the C gauge [45, 46]. There is no unique Eulerian frame in GR, but a convenient choice is the total-matter (T) gauge. This is related to the C gauge by a purely spatial transformation, so that at first order, the matter and galaxy overdensities are the same [45]:

$$\delta_{mC}^{(1)} = \delta_{mT}^{(1)}, \quad \delta_{gC}^{(1)} = \delta_{gT}^{(1)} = b_1\delta_{mT}^{(1)}. \quad (18)$$

The last equality is the definition of the Eulerian bias parameter at first order. This means that b_1 in (16) is the Eulerian bias parameter.

We extend (16) to higher order with the simplest possible model of scale-independent bias. This model assumes that galaxy number density contrast is a local function of only the matter density contrast – the so-called local-in-mass-density model. For a physical definition valid on ultra-large scales, we require that the bias coefficients are scale-independent in the galaxy rest-frame, i.e. in C gauge. Expanding in powers of the mass density contrast, we have

$$\delta_{gC} = b_1 \delta_{mC} + \frac{1}{2} b_2 (\delta_{mC})^2 + \dots, \quad (19)$$

where $b_I = b_I(a, \ln L)$. At first order, this recovers (16). At second order we have:²

$$\delta_{gC}^{(2)} = b_1 \delta_{mC}^{(2)} + b_2 [\delta_{mC}^{(1)}]^2. \quad (20)$$

The relation between C- and T-gauge matter overdensities at second order is [45, 46]

$$\delta_{mT}^{(2)} = \delta_{mC}^{(2)} + 2[\partial_i \delta_{mC}^{(1)}] \nabla^{-2} \partial^i \delta_{mC}^{(1)}, \quad (21)$$

where $-2\nabla^{-2} \partial^i \delta_{mC}^{(1)}$ is a gauge generator. Since the C \rightarrow T gauge transformation is purely spatial, (21) also applies to the galaxy counts:

$$\delta_{gT}^{(2)} = \delta_{gC}^{(2)} + 2[\partial_i \delta_{gC}^{(1)}] \nabla^{-2} \partial^i \delta_{mC}^{(1)}. \quad (22)$$

From (20)–(22), using (18), we find that

$$\begin{aligned} \delta_{gT}^{(2)} &= b_1 \delta_{mC}^{(2)} + b_2 [\delta_{mC}^{(1)}]^2 + 2b_1 [\partial_i \delta_{mC}^{(1)}] \nabla^{-2} \partial^i \delta_{mC}^{(1)} \\ &= b_1 \left[\delta_{mC}^{(2)} + 2[\partial_i \delta_{mT}^{(1)}] \nabla^{-2} \partial^i \delta_{mC}^{(1)} \right] + b_2 [\delta_{mC}^{(1)}]^2 \end{aligned} \quad (23)$$

which implies

$$\delta_{gT}^{(2)} = b_1 \delta_{mT}^{(2)} + b_2 [\delta_{mT}^{(1)}]^2. \quad (24)$$

Therefore local-in-mass-density and scale-independent bias in C and T gauge are equivalent up to second order, with the same Eulerian bias coefficients.

We will use the T gauge, since the relation to the Poisson gauge overdensity is simpler for T gauge than C gauge. In Appendix A, we show that

$$\begin{aligned} \delta_g^{(2)} &= \delta_{gT}^{(2)} + (3 - b_e) \mathcal{H} v^{(2)} + 2(3 - b_e) \mathcal{H} v^{(1)} \delta_{gT}^{(1)} - 2v^{(1)} \delta_{gT}^{(1)'} \\ &\quad + \left[(b_e - 3) \mathcal{H}' + b_e' \mathcal{H} + (b_e - 3)^2 \mathcal{H}^2 \right] [v^{(1)}]^2 + (b_e - 3) \mathcal{H} v^{(1)} v^{(1)'} \\ &\quad - (b_e - 3) \mathcal{H} \nabla^{-2} \left[v^{(1)} \nabla^2 v^{(1)'} - v^{(1)'} \nabla^2 v^{(1)} - 6\partial_i \Phi^{(1)} \partial^i v^{(1)} - 6\Phi^{(1)} \nabla^2 v^{(1)} \right]. \end{aligned} \quad (25)$$

By (16) and (24), this leads to the final expression for the Poisson-gauge galaxy density contrast in the simplest local bias model:

$$\begin{aligned} \delta_g^{(2)} &= b_1 \delta_{mT}^{(2)} + b_2 [\delta_{mT}^{(1)}]^2 + \left[(b_e - 3)^2 \mathcal{H}^2 + b_e' \mathcal{H} + (b_e - 3) \mathcal{H}' \right] [v^{(1)}]^2 + (b_e - 3) \mathcal{H} v^{(1)} v^{(1)'} + 2b_1 (3 - b_e) \mathcal{H} v^{(1)} \delta_{mT}^{(1)} \\ &\quad - 2v^{(1)} \left[b_1 \delta_{mT}^{(1)'} + b_1' \delta_{mT}^{(1)} \right] + (3 - b_e) \mathcal{H} \nabla^{-2} \left[v^{(1)} \nabla^2 v^{(1)'} - v^{(1)'} \nabla^2 v^{(1)} - 6\partial_i \Phi^{(1)} \partial^i v^{(1)} - 6\Phi^{(1)} \nabla^2 v^{(1)} \right]. \end{aligned} \quad (26)$$

The velocity and metric potential terms ensure gauge-independence on ultra-large scales. Equation (26) is the second-order generalisation of (17).

² For convenience, we have omitted the term $-b_2 \langle [\delta_{mC}^{(1)}]^2 \rangle$ on the right of (20).

II.2. Observed galaxy number counts in Poisson gauge

At first order, we replace $\delta_g^{(1)}$ using the bias relations (16)–(18), and then split $\Delta_g^{(1)}$ into Newtonian and GR parts:

$$\Delta_{gN}^{(1)} = b_1 \delta_{mT}^{(1)} - \frac{1}{\mathcal{H}} \partial_{\parallel}^2 v^{(1)}, \quad (27)$$

$$\Delta_{gGR}^{(1)} = \left[b_e - 2\mathcal{Q} + \frac{2(\mathcal{Q} - 1)}{\chi\mathcal{H}} - \frac{\mathcal{H}'}{\mathcal{H}^2} \right] \left[\partial_{\parallel} v^{(1)} - \Phi^{(1)} \right] + (2\mathcal{Q} - 1) \Phi^{(1)} + \frac{1}{\mathcal{H}} \Phi^{(1)'} + (3 - b_e) \mathcal{H} v^{(1)}. \quad (28)$$

The Newtonian part = T-gauge density contrast + Kaiser RSD, and the GR part = Doppler + potential + velocity potential. The velocity potential arises from the term in (17), which may be expressed in terms of the metric potential via (14) and (15). The Doppler term in (28) is the one proportional to the line-of-sight velocity $\partial_{\parallel} v^{(1)}$.

At second order, we use the gauge-independent bias model (26) to replace the Poisson-gauge $\delta_g^{(2)}$ term in $\Delta_g^{(2)}$. The remaining terms in $\Delta_g^{(2)}$ are second-order generalisations of RSD, Doppler and potential terms, together with quadratic couplings amongst all the first-order terms. The quadratic terms encode an interaction between two effects; in Fourier space, they correspond to mode coupling.

The general equation for $\Delta_g^{(2)}$, including evolution bias and magnification bias, as well as all integrated effects, is given in [29] (including recent corrections [47]). We include in this general expression our gauge-independent model of the galaxy bias at second order, (26), and we neglect the terms with integrated contributions. The result is

$$\begin{aligned} \Delta_g^{(2)} = & b_1 \delta_{mT}^{(2)} + b_2 [\delta_{mT}^{(1)}]^2 + \left[(b_e - 3)^2 \mathcal{H}^2 + b_e' \mathcal{H} + (b_e - 3) \mathcal{H}' \right] [v^{(1)}]^2 + (b_e - 3) \mathcal{H} v^{(1)} v^{(1)'} + 2b_1 (3 - b_e) \mathcal{H} v^{(1)} \delta_{mT}^{(1)} \\ & - 2v^{(1)} \left[b_1 \delta_{mT}^{(1)'} + b_1' \delta_{mT}^{(1)} \right] + (3 - b_e) \mathcal{H} \nabla^{-2} \left[v^{(1)} \nabla^2 v^{(1)'} - v^{(1)'} \nabla^2 v^{(1)} - 6\partial_i \Phi^{(1)} \partial^i v^{(1)} - 6\Phi^{(1)} \nabla^2 v^{(1)} \right] \\ & - \frac{1}{\mathcal{H}} \partial_{\parallel}^2 v^{(2)} + (3 - b_e) \mathcal{H} v^{(2)} + \left[b_e - 2\mathcal{Q} - \frac{2(1 - \mathcal{Q})}{\chi\mathcal{H}} - \frac{\mathcal{H}'}{\mathcal{H}^2} \right] \left[\partial_{\parallel} v^{(2)} - \Phi^{(2)} \right] + 2(\mathcal{Q} - 1) \Psi^{(2)} + \Phi^{(2)} + \frac{1}{\mathcal{H}} \Psi^{(2)'} \\ & + \left[b_e - 2\mathcal{Q} - \frac{\mathcal{H}'}{\mathcal{H}^2} - (1 - \mathcal{Q}) \frac{2}{\chi\mathcal{H}} \right] \left[3[\Phi^{(1)}]^2 - [\partial_{\parallel} v^{(1)}]^2 + \partial_{\perp i} v^{(1)} \partial_{\perp}^i v^{(1)} - 2\partial_{\parallel} v^{(1)} \Phi^{(1)} \right] \\ & - \frac{2}{\mathcal{H}} \left(\Phi^{(1)} - \partial_{\parallel} v^{(1)} \right) \left(\Phi^{(1)'} - \partial_{\parallel}^2 v^{(1)} \right) \left. \right] + 2(2\mathcal{Q} - 1) \Phi^{(1)} \delta_g^{(1)} - \frac{2}{\mathcal{H}} \delta_g^{(1)} \partial_{\parallel}^2 v^{(1)} + \frac{2}{\mathcal{H}} \delta_g^{(1)} \Phi^{(1)'} \\ & + \left(4\mathcal{Q} - 5 + 4\mathcal{Q}^2 - 4 \frac{\partial\mathcal{Q}}{\partial \ln \bar{L}} \right) [\Phi^{(1)}]^2 + \frac{2}{\mathcal{H}} \left(2\mathcal{Q} + \frac{\mathcal{H}'}{\mathcal{H}^2} \right) \Phi^{(1)} \Phi^{(1)'} \\ & - \frac{2}{\mathcal{H}} \left(1 + 2\mathcal{Q} + \frac{\mathcal{H}'}{\mathcal{H}^2} \right) \Phi^{(1)} \partial_{\parallel}^2 v^{(1)} + \frac{2}{\mathcal{H}^2} [\Phi^{(1)'}]^2 + \frac{2}{\mathcal{H}^2} [\partial_{\parallel}^2 v^{(1)}]^2 + \frac{2}{\mathcal{H}^2} \partial_{\parallel} v^{(1)} \partial_{\parallel}^2 \Phi^{(1)} + \frac{4}{\mathcal{H}} \partial_{\parallel} v^{(1)} \partial_{\parallel} \Phi^{(1)} \\ & - \frac{2}{\mathcal{H}^2} \Phi^{(1)} \partial_{\parallel}^3 v^{(1)} - \frac{2}{\mathcal{H}} \Phi^{(1)} \partial_{\parallel} \Phi^{(1)} + \frac{2}{\mathcal{H}^2} \Phi^{(1)} \frac{d\Phi^{(1)'}}{d\chi} - \frac{2}{\mathcal{H}^2} \partial_{\parallel} v^{(1)} \frac{d\Phi^{(1)'}}{d\chi} + \frac{2}{\mathcal{H}} \left(1 + \frac{\mathcal{H}'}{\mathcal{H}^2} \right) \partial_{\parallel} v^{(1)} \partial_{\parallel}^2 v^{(1)} \\ & - \frac{2}{\mathcal{H}^2} \Phi^{(1)} \partial_{\parallel}^2 \Phi^{(1)} + \frac{2}{\mathcal{H}} \left(1 - \frac{\mathcal{H}'}{\mathcal{H}^2} \right) \partial_{\parallel} v^{(1)} \Phi^{(1)'} - \frac{4}{\mathcal{H}^2} \partial_{\parallel}^2 v^{(1)} \Phi^{(1)'} + \frac{2}{\mathcal{H}} \partial_{\perp i} v^{(1)} \partial_{\perp}^i \Phi^{(1)} - \frac{4}{\mathcal{H}} \partial_{\perp i} v^{(1)} \partial_{\perp}^i \partial_{\parallel} v^{(1)} \\ & + \left(\frac{4}{\chi\mathcal{H}} - 1 \right) \partial_{\perp i} v^{(1)} \partial_{\perp}^i v^{(1)} + \frac{2}{\mathcal{H}^2} \partial_{\parallel} v^{(1)} \partial_{\parallel}^3 v^{(1)} + \left\{ \left[4b_e \mathcal{Q} - 2b_e - 4\mathcal{Q} - 8\mathcal{Q}^2 + 8 \frac{\partial\mathcal{Q}}{\partial \ln \bar{L}} + 4 \frac{\partial\mathcal{Q}}{\partial \ln \bar{a}} \right. \right. \\ & + 2 \frac{\mathcal{H}'}{\mathcal{H}^2} (1 - 2\mathcal{Q}) + \frac{4}{\chi\mathcal{H}} \left(\mathcal{Q} - 1 + 2\mathcal{Q}^2 - 2 \frac{\partial\mathcal{Q}}{\partial \ln \bar{L}} \right) \left. \right] \Phi^{(1)} + 2 \left[b_e - 2\mathcal{Q} - \frac{\mathcal{H}'}{\mathcal{H}^2} - \frac{2}{\chi\mathcal{H}} (1 - \mathcal{Q}) \right] \delta_g^{(1)} \\ & - \frac{2}{\mathcal{H}} \frac{d\delta_g^{(1)}}{d\chi} + \frac{2}{\mathcal{H}} \left[2\mathcal{Q} - b_e + \frac{\mathcal{H}'}{\mathcal{H}^2} + \frac{2}{\chi\mathcal{H}} (1 - \mathcal{Q}) \right] \partial_{\parallel}^2 v^{(1)} + \frac{2}{\mathcal{H}} \left[b_e - 2 - \frac{2}{\chi\mathcal{H}} (1 - \mathcal{Q}) \right. \\ & - \left. \frac{\mathcal{H}'}{\mathcal{H}^2} \right] \Phi^{(1)'} - \frac{4}{\mathcal{H}} \mathcal{Q} \partial_{\parallel} \Phi \left. \right\} \left[\partial_{\parallel} v^{(1)} - \Phi^{(1)} \right] + \left\{ b_e^2 - b_e + \frac{\partial b_e}{\partial \ln \bar{a}} + 6\mathcal{Q} - 4\mathcal{Q} b_e + 4\mathcal{Q}^2 - 4 \frac{\partial\mathcal{Q}}{\partial \ln \bar{L}} - 4 \frac{\partial\mathcal{Q}}{\partial \ln \bar{a}} \right. \\ & + \frac{6}{\chi} \frac{\mathcal{H}'}{\mathcal{H}^3} (1 - \mathcal{Q}) + (1 - 2b_e + 4\mathcal{Q}) \frac{\mathcal{H}'}{\mathcal{H}^2} - \frac{\mathcal{H}''}{\mathcal{H}^3} + 3 \frac{\mathcal{H}'^2}{\mathcal{H}^4} + \frac{2}{\chi^2 \mathcal{H}^2} \left(1 - \mathcal{Q} + 2\mathcal{Q}^2 - 2 \frac{\partial\mathcal{Q}}{\partial \ln \bar{L}} \right) + \frac{2}{\chi\mathcal{H}} \left[1 - 2b_e - \mathcal{Q} \right. \\ & \left. \left. + 2b_e \mathcal{Q} - 4\mathcal{Q}^2 + 4 \frac{\partial\mathcal{Q}}{\partial \ln \bar{L}} + 2 \frac{\partial\mathcal{Q}}{\partial \ln \bar{a}} \right] \right\} \left[\partial_{\parallel} v^{(1)} - \Phi^{(1)} \right]^2 + 4 \left[\left(1 - \frac{1}{\chi\mathcal{H}} \right) \partial_{\parallel} v^{(1)} - \left(2 - \frac{1}{\chi\mathcal{H}} \right) \Phi^{(1)} \right] \frac{\partial \delta_g^{(1)}}{\partial \ln \bar{L}}. \quad (29) \end{aligned}$$

The Newtonian part of (29) is formed from the density contrast and Kaiser RSD terms and their couplings:³

$$\Delta_{gN}^{(2)} = b_1 \delta_{mT}^{(2)} + b_2 [\delta_{mT}^{(1)}]^2 - \frac{1}{\mathcal{H}} \partial_{\parallel}^2 v^{(2)} - 2 \frac{b_1}{\mathcal{H}} \left[\delta_{mT}^{(1)} \partial_{\parallel}^2 v^{(1)} + \partial_{\parallel} v^{(1)} \partial_{\parallel} \delta_{mT}^{(1)} \right] + \frac{2}{\mathcal{H}^2} \left[[\partial_{\parallel}^2 v^{(1)}]^2 + \partial_{\parallel} v^{(1)} \partial_{\parallel}^3 v^{(1)} \right]. \quad (30)$$

The remaining terms form the GR correction:

$$\begin{aligned} \Delta_{gGR}^{(2)} = & \mathcal{H}(3 - b_e)v^{(2)} + \left[(9 - 6b_e + b_e^2)\mathcal{H}^2 + b'_e\mathcal{H} + (b_e - 3)\mathcal{H}' \right] [v^{(1)}]^2 + (b_e - 3)\mathcal{H}v^{(1)}v^{(1)'} \\ & - (b_e - 3)\mathcal{H}\nabla^{-2} \left[v^{(1)}\nabla^2 v^{(1)'} - v^{(1)'}\nabla^2 v^{(1)} - 6\partial_i\Phi^{(1)}\partial^i v^{(1)} - 6\Phi^{(1)}\nabla^2 v^{(1)} \right] + 2(3 - b_e)b_1\mathcal{H}v^{(1)}\delta_{mT}^{(1)} \\ & - 2v^{(1)} \left(b'_1\delta_{mT}^{(1)} + b_1\delta_{mT}^{(1)'} \right) + \left[b_e - 2\mathcal{Q} - \frac{2(1 - \mathcal{Q})}{\chi\mathcal{H}} - \frac{\mathcal{H}'}{\mathcal{H}^2} \right] \partial_{\parallel} v^{(2)} + \left[1 - b_e + 2\mathcal{Q} + \frac{2(1 - \mathcal{Q})}{\chi\mathcal{H}} + \frac{\mathcal{H}'}{\mathcal{H}^2} \right] \Phi^{(2)} \\ & - 2(1 - \mathcal{Q})\Psi^{(2)} + \frac{1}{\mathcal{H}}\Psi^{(2)'} + \frac{2}{\mathcal{H}} \left[b_1\delta_{mT}^{(1)'}\partial_{\parallel} v^{(1)} + (f - 2 + 2\mathcal{Q})\Phi^{(1)}\partial_{\parallel}\Phi^{(1)} + (2 - f - 2\mathcal{Q})\partial_{\parallel}v^{(1)}\partial_{\parallel}\Phi^{(1)} \right. \\ & \left. - b_1\Phi^{(1)}\delta_{mT}^{(1)'} + b_1\Phi^{(1)}\partial_{\parallel}\delta_{mT}^{(1)} - 2\partial_i v^{(1)}\partial_{\parallel}\partial^i v^{(1)} + \partial_i v^{(1)}\partial^i\Phi^{(1)} \right] + \frac{2}{\mathcal{H}^2} \left[\partial_{\parallel}v^{(1)}\partial_{\parallel}^2\Phi^{(1)} - \Phi^{(1)}\partial_{\parallel}^2\Phi^{(1)} - \Phi^{(1)}\partial_{\parallel}^3v^{(1)} \right] \\ & - 2(3 - b_e)v^{(1)}\partial_{\parallel}^2 v^{(1)} + 2 \left[b_1 \left(b_e - 2\mathcal{Q} - \frac{2(1 - \mathcal{Q})}{\chi\mathcal{H}} - \frac{\mathcal{H}'}{\mathcal{H}^2} \right) + \frac{b'_1}{\mathcal{H}} + 2 \left(1 - \frac{1}{\chi\mathcal{H}} \right) \frac{\partial b_1}{\partial \ln \bar{L}} \right] \delta_{mT}^{(1)}\partial_{\parallel} v^{(1)} \\ & + \frac{2}{\mathcal{H}} \left[3 - 2b_e + 4\mathcal{Q} + \frac{4(1 - \mathcal{Q})}{\mathcal{H}\chi} + \frac{3\mathcal{H}'}{\mathcal{H}} \right] \partial_{\parallel}v^{(1)}\partial_{\parallel}^2 v^{(1)} + 2 \left[b_1 \left(f - 2 - b_e + 4\mathcal{Q} + \frac{2(1 - \mathcal{Q})}{\chi\mathcal{H}} + \frac{\mathcal{H}'}{\mathcal{H}^2} \right) - \frac{b'_1}{\mathcal{H}} \right. \\ & \left. - 2 \left(2 - \frac{1}{\chi\mathcal{H}} \right) \frac{\partial b_1}{\partial \ln \bar{L}} \right] \Phi^{(1)}\delta_{mT}^{(1)} + \left[b_e - 1 - 2\mathcal{Q} - \frac{2(1 - \mathcal{Q})}{\chi\mathcal{H}} - \frac{\mathcal{H}'}{\mathcal{H}^2} \right] \partial_i v^{(1)}\partial^i v^{(1)} + \frac{2}{\mathcal{H}} \left[1 - 2f + 2b_e - 6\mathcal{Q} \right. \\ & \left. - \frac{4(1 - \mathcal{Q})}{\chi\mathcal{H}} - \frac{3\mathcal{H}'}{\mathcal{H}^2} \right] \Phi^{(1)}\partial_{\parallel}^2 v^{(1)} + \mathcal{A}[\Phi^{(1)}]^2 + \mathcal{B}v^{(1)}\partial_{\parallel}v^{(1)} + \mathcal{C}\Phi^{(1)}v^{(1)} + \mathcal{D}\Phi^{(1)}\partial_{\parallel}v^{(1)} + \mathcal{E}[\partial_{\parallel}v^{(1)}]^2. \quad (31) \end{aligned}$$

The background coefficients in the last line are

$$\begin{aligned} \mathcal{A} = & -3 + 2f \left(2 - 2b_e + 4\mathcal{Q} + \frac{4(1 - \mathcal{Q})}{\chi\mathcal{H}} + \frac{2\mathcal{H}'}{\mathcal{H}^2} \right) - \frac{2f'}{\mathcal{H}} + b_e^2 + 6b_e - 8b_e\mathcal{Q} + 4\mathcal{Q} + 16\mathcal{Q}^2 - 16 \frac{\partial\mathcal{Q}}{\partial \ln \bar{L}} \\ & - 8 \frac{\mathcal{Q}'}{\mathcal{H}} + \frac{b'_e}{\mathcal{H}} + \frac{2}{\chi^2\mathcal{H}^2} \left(1 - \mathcal{Q} + 2\mathcal{Q}^2 - 2 \frac{\partial\mathcal{Q}}{\partial \ln \bar{L}} \right) - \frac{2}{\chi\mathcal{H}} \left[4 + 2b_e - 2b_e\mathcal{Q} - 4\mathcal{Q} + 8\mathcal{Q}^2 - \frac{3\mathcal{H}'}{\mathcal{H}^2}(1 - \mathcal{Q}) \right. \\ & \left. - 8 \frac{\partial\mathcal{Q}}{\partial \ln \bar{L}} - 2 \frac{\mathcal{Q}'}{\mathcal{H}} \right] + \frac{\mathcal{H}'}{\mathcal{H}^2} \left(-8 - 2b_e + 8\mathcal{Q} + \frac{3\mathcal{H}'}{\mathcal{H}^2} \right) - \frac{\mathcal{H}''}{\mathcal{H}^3}, \quad (32) \end{aligned}$$

$$\mathcal{B} = 2\mathcal{H} \left[-3 + 4b_e + 2b_e \frac{(1 - \mathcal{Q})}{\chi\mathcal{H}} - b_e^2 + 2b_e\mathcal{Q} - 6\mathcal{Q} - \frac{b'_e}{\mathcal{H}} - \frac{6(1 - \mathcal{Q})}{\chi\mathcal{H}} + 2 \left(1 - \frac{1}{\chi\mathcal{H}} \right) \frac{\mathcal{Q}'}{\mathcal{H}} \right], \quad (33)$$

$$\mathcal{C} = 2\mathcal{H} \left[-3 + f(3 - b_e) - 3b_e - 2b_e \frac{(1 - \mathcal{Q})}{\chi\mathcal{H}} + \frac{b'_e}{\mathcal{H}} + b_e^2 - 4b_e\mathcal{Q} + 12\mathcal{Q} + \frac{6(1 - \mathcal{Q})}{\chi\mathcal{H}} - 2 \left(2 - \frac{1}{\chi\mathcal{H}} \right) \frac{\mathcal{Q}'}{\mathcal{H}} \right], \quad (34)$$

$$\begin{aligned} \mathcal{D} = & 4 + 2f \left[-3 + f + 2b_e - 3\mathcal{Q} - \frac{4(1 - \mathcal{Q})}{\chi\mathcal{H}} - \frac{2\mathcal{H}'}{\mathcal{H}^2} \right] + \frac{2f'}{\mathcal{H}} - 6b_e - 2b_e^2 + 12b_e\mathcal{Q} - 8\mathcal{Q} - 16\mathcal{Q}^2 + 16 \frac{\partial\mathcal{Q}}{\partial \ln \bar{L}} \\ & + 12 \frac{\mathcal{Q}'}{\mathcal{H}} - 2 \frac{b'_e}{\mathcal{H}} - \frac{4}{\chi^2\mathcal{H}^2} \left(1 - \mathcal{Q} + 2\mathcal{Q}^2 - 2 \frac{\partial\mathcal{Q}}{\partial \ln \bar{L}} \right) - \frac{4}{\chi\mathcal{H}} \left[-1 - 2b_e + 2b_e\mathcal{Q} + \mathcal{Q} - 6\mathcal{Q}^2 + \frac{3\mathcal{H}'}{\mathcal{H}^2}(1 - \mathcal{Q}) \right. \\ & \left. + 6 \frac{\partial\mathcal{Q}}{\partial \ln \bar{L}} + 2 \frac{\mathcal{Q}'}{\mathcal{H}} \right] + \frac{2\mathcal{H}'}{\mathcal{H}^2} \left(3 + 2b_e - 6\mathcal{Q} - \frac{3\mathcal{H}'}{\mathcal{H}^2} \right) + \frac{2\mathcal{H}''}{\mathcal{H}^3}, \quad (35) \end{aligned}$$

$$\begin{aligned} \mathcal{E} = & -4 - b_e + b_e^2 - 4b_e\mathcal{Q} + 6\mathcal{Q} + 4\mathcal{Q}^2 - 4 \frac{\partial\mathcal{Q}}{\partial \ln \bar{L}} - 4 \frac{\mathcal{Q}'}{\mathcal{H}} + \frac{b'_e}{\mathcal{H}} + \frac{2}{\chi^2\mathcal{H}^2} \left(1 - \mathcal{Q} + 2\mathcal{Q}^2 - 2 \frac{\partial\mathcal{Q}}{\partial \ln \bar{L}} \right) \\ & + \frac{2}{\chi\mathcal{H}} \left[3 - 2b_e + 2b_e\mathcal{Q} - 3\mathcal{Q} - 4\mathcal{Q}^2 + \frac{3\mathcal{H}'}{\mathcal{H}^2}(1 - \mathcal{Q}) + 4 \frac{\partial\mathcal{Q}}{\partial \ln \bar{L}} + 2 \frac{\mathcal{Q}'}{\mathcal{H}} \right] + \frac{\mathcal{H}'}{\mathcal{H}^2} \left(3 - 2b_e + 4\mathcal{Q} + \frac{3\mathcal{H}'}{\mathcal{H}^2} \right) - \frac{\mathcal{H}''}{\mathcal{H}^3}. \quad (36) \end{aligned}$$

³ Note that the GR correction to $\delta_{mT}^{(2)}$ does *not* enter the bias term $b_1\delta_{mT}^{(2)}$, as explained in [48–50]. There is a GR correction to $v^{(2)}$, which we neglect here.

In deriving (30)–(36) from (29), we used the following:

- (a) eliminate $d/d\chi$ using (9), and $\partial_{\perp i}$ using (8);
- (b) show, using the commutator relation $[\partial_{\perp i}, \partial_{\parallel}] = \chi^{-1} \partial_{\perp i}$, that

$$\partial_{\perp i} v^{(1)} \partial_{\perp}^i \partial_{\parallel} v^{(1)} = \partial_i v^{(1)} \partial_{\parallel} \partial^i v^{(1)} - \partial_{\parallel} v^{(1)} \partial_{\parallel}^2 v^{(1)} + \frac{1}{\chi} [\partial_i v^{(1)} \partial^i v^{(1)} - [\partial_{\parallel} v^{(1)}]^2]; \quad (37)$$

- (c) express $\delta_g^{(1)}$ in terms of $\delta_{mT}^{(1)}$ and $v^{(1)}$, using (17) and (18);
- (d) rewrite the term from the perturbation of the magnification bias, using (16)–(18), as

$$\frac{\partial \delta_g^{(1)}}{\partial \ln \bar{L}} = \frac{\partial b_1}{\partial \ln \bar{L}} \delta_{mT}^{(1)} - \frac{\partial b_e}{\partial \ln \bar{L}} \mathcal{H} v^{(1)} = \frac{\partial b_1}{\partial \ln \bar{L}} \delta_{mT}^{(1)} + \mathcal{Q}' v^{(1)}, \quad (38)$$

where the second equality uses (6), (7) and $\partial/\partial \ln a = \mathcal{H}^{-1} \partial/\partial \eta$.

In summary: we have used the general formula for $\Delta_g^{(2)}$ in Poisson gauge, given in [29], neglecting the terms with line-of-sight integrals, to derive (30)–(36). In these equations we have broken down the highly complex formula in [29] into simple parts, facilitating analytical and then numerical analysis. Our new contribution is to determine the Poisson-gauge $\delta_g^{(2)}$ via a simple local-in-mass-density model of bias (26), that is gauge independent and valid on ultra-large scales.⁴

⁴ Three groups have computed $\Delta_g^{(2)}$ – in [29–31], [32] and [33]. All have used different formalisms. The collective task of cross-checking these independent results has been initiated but is not complete, even in the simplest case with no integrated contributions and $b_e = 0 = \mathcal{Q}$.

III. GALAXY NUMBER OVERDENSITY IN FOURIER SPACE AND THE BISPECTRUM

We will only consider correlations at the same observed redshift. At fixed redshift z , the perturbative variables depend on \mathbf{n} and can be computed in Fourier space at fixed $\eta(z)$. With \mathbf{n} and z fixed, we transform $\mathbf{x} = [\eta_0 - \eta(z)]\mathbf{n} + \mathbf{x}_0 \rightarrow \mathbf{k}$, which is equivalent to transforming over all observer positions \mathbf{x}_0 . Our Fourier convention is

$$f(\mathbf{x}) = \int \frac{d^3k}{(2\pi)^3} e^{i\mathbf{k}\cdot\mathbf{x}} f(\mathbf{k}), \quad f(\mathbf{k}) = \int d^3x e^{-i\mathbf{k}\cdot\mathbf{x}} f(\mathbf{x}) = \int \frac{d^3k'}{(2\pi)^3} (2\pi)^3 \delta^D(\mathbf{k} - \mathbf{k}') f(\mathbf{k}'), \quad (39)$$

where we suppress the redshift dependence. The transform of a product $h(\mathbf{x}) = g(\mathbf{x})f(\mathbf{x})$ leads to a convolution in Fourier space

$$h(\mathbf{k}) = \int \frac{d^3k_1}{(2\pi)^3} \frac{d^3k_2}{(2\pi)^3} f(\mathbf{k}_1)g(\mathbf{k}_2)(2\pi)^3 \delta^D(\mathbf{k}_1 + \mathbf{k}_2 - \mathbf{k}). \quad (40)$$

For notational convenience we write the T-gauge matter density contrast as

$$\delta_{mT} \equiv \delta = \delta^{(1)} + \frac{1}{2}\delta^{(2)}, \quad (41)$$

from now on.

At second order, the matter density contrast and the velocity and metric potentials are given in a Newtonian approximation by [51]:

$$\delta^{(2)}(\mathbf{k}) = \int \frac{d^3k_1}{(2\pi)^3} \frac{d^3k_2}{(2\pi)^3} \delta^{(1)}(\mathbf{k}_1)\delta^{(1)}(\mathbf{k}_2)F_2(\mathbf{k}_1, \mathbf{k}_2)(2\pi)^3 \delta^D(\mathbf{k}_1 + \mathbf{k}_2 - \mathbf{k}), \quad (42)$$

$$v^{(2)}(\mathbf{k}) = f \frac{\mathcal{H}}{k^2} \int \frac{d^3k_1}{(2\pi)^3} \frac{d^3k_2}{(2\pi)^3} \delta^{(1)}(\mathbf{k}_1)\delta^{(1)}(\mathbf{k}_2)G_2(\mathbf{k}_1, \mathbf{k}_2)(2\pi)^3 \delta^D(\mathbf{k}_1 + \mathbf{k}_2 - \mathbf{k}), \quad (43)$$

$$\Phi^{(2)}(\mathbf{k}) = \Psi^{(2)}(\mathbf{k}) = -\frac{3}{2}\Omega_m \frac{\mathcal{H}^2}{k^2} \delta^{(2)}(\mathbf{k}). \quad (44)$$

The kernels for the dark matter and peculiar velocity perturbations in a matter-dominated model are

$$F_2(\mathbf{k}_1, \mathbf{k}_2) = \frac{10}{7} + \frac{\mathbf{k}_1 \cdot \mathbf{k}_2}{k_1 k_2} \left(\frac{k_1}{k_2} + \frac{k_2}{k_1} \right) + \frac{4}{7} \left(\frac{\mathbf{k}_1 \cdot \mathbf{k}_2}{k_1 k_2} \right)^2, \quad (45)$$

$$G_2(\mathbf{k}_1, \mathbf{k}_2) = \frac{6}{7} + \frac{\mathbf{k}_1 \cdot \mathbf{k}_2}{k_1 k_2} \left(\frac{k_1}{k_2} + \frac{k_2}{k_1} \right) + \frac{8}{7} \left(\frac{\mathbf{k}_1 \cdot \mathbf{k}_2}{k_1 k_2} \right)^2. \quad (46)$$

The corrections to these kernels from the presence of Λ are small [35], and we neglect them. Within the same approximation, we have $\delta^{(2)} \propto D^2 \delta_0^{(2)}$, so that $\delta^{(2)'} = 2f\mathcal{H}\delta^{(2)}$. Then it follows from (44) that

$$\Phi^{(2)'} = (2f - 1)\mathcal{H}\Phi^{(2)}. \quad (47)$$

We write $\Delta_g^{(1,2)}$ in terms of kernels:

$$\Delta_g^{(1)}(\mathbf{k}_2) = \int \frac{d^3k_1}{(2\pi)^3} \mathcal{K}^{(1)}(\mathbf{k}_1)\delta^{(1)}(\mathbf{k}_1)(2\pi)^3 \delta^D(\mathbf{k}_1 - \mathbf{k}_2), \quad (48)$$

$$\Delta_g^{(2)}(\mathbf{k}_3) = \int \frac{d^3k_1}{(2\pi)^3} \frac{d^3k_2}{(2\pi)^3} \mathcal{K}^{(2)}(\mathbf{k}_1, \mathbf{k}_2, \mathbf{k}_3)\delta^{(1)}(\mathbf{k}_1)\delta^{(1)}(\mathbf{k}_2)(2\pi)^3 \delta^D(\mathbf{k}_1 + \mathbf{k}_2 - \mathbf{k}_3) - \delta^{(D)}(\mathbf{k}_3)\langle \Delta_g^{(2)} \rangle, \quad (49)$$

and we split the kernels into Newtonian and GR parts, $\mathcal{K}^{(1,2)} = \mathcal{K}_N^{(1,2)} + \mathcal{K}_{GR}^{(1,2)}$. In (49), we subtracted off the ensemble average of Δ_g :

$$\langle \Delta_g^{(2)} \rangle = \int \frac{d^3k_1}{(2\pi)^3} P(k_1)\mathcal{K}^{(2)}(\mathbf{k}_1, -\mathbf{k}_1, 0), \quad (50)$$

in order to ensure that $\langle \Delta_g \rangle = 0$. Here $P(k) \equiv P_{\delta^{(1)}}(k)$ is the linear matter power spectrum.

By (27) and (28), the linear order kernel is given by

$$\mathcal{K}_N^{(1)}(\mathbf{k}) = b_1 + f\mu^2, \quad \mathcal{K}_{\text{GR}}^{(1)}(\mathbf{k}) = i\frac{\mu}{k}\gamma_1 + \frac{\gamma_2}{k^2}, \quad \mu = \hat{\mathbf{k}} \cdot \mathbf{n}, \quad (51)$$

where γ_1 and γ_2 are redshift dependent:

$$\frac{\gamma_1}{\mathcal{H}} = f \left[b_e - 2\mathcal{Q} - \frac{2(1-\mathcal{Q})}{\chi\mathcal{H}} - \frac{\mathcal{H}'}{\mathcal{H}^2} \right], \quad (52)$$

$$\frac{\gamma_2}{\mathcal{H}^2} = f(3 - b_e) + \frac{3}{2}\Omega_m \left[2 + b_e - f - 4\mathcal{Q} - 2\frac{(1-\mathcal{Q})}{\chi\mathcal{H}} - \frac{\mathcal{H}'}{\mathcal{H}^2} \right]. \quad (53)$$

At second order, the Newtonian part of the kernel is

$$\begin{aligned} \mathcal{K}_N^{(2)}(\mathbf{k}_1, \mathbf{k}_2, \mathbf{k}_3) &= b_1 F_2(\mathbf{k}_1, \mathbf{k}_2) + b_2 + f G_2(\mathbf{k}_1, \mathbf{k}_2) \mu_3^2 \\ &+ f^2 \frac{\mu_1 \mu_2}{k_1 k_2} (\mu_1 k_1 + \mu_2 k_2)^2 + b_1 \frac{f}{k_1 k_2} \left[(\mu_1^2 + \mu_2^2) k_1 k_2 + \mu_1 \mu_2 (k_1^2 + k_2^2) \right], \end{aligned} \quad (54)$$

where $\mu_i = \hat{\mathbf{k}}_i \cdot \mathbf{n}$. The second line in (54) is the nonlinear Kaiser RSD contribution [20, 21].

The GR part follows from (31), after transformation to Fourier space. The details, with all the necessary transforms, are given in Appendix B, and they lead to the GR kernel:

$$\begin{aligned} \mathcal{K}_{\text{GR}}^{(2)}(\mathbf{k}_1, \mathbf{k}_2, \mathbf{k}_3) &= \frac{1}{k_1^2 k_2^2} \left\{ \Gamma_1 + i(\mu_1 k_1 + \mu_2 k_2) \Gamma_2 + \frac{k_1^2 k_2^2}{k_3^2} \left[F_2(\mathbf{k}_1, \mathbf{k}_2) \Gamma_3 + G_2(\mathbf{k}_1, \mathbf{k}_2) \Gamma_4 \right] \right. \\ &+ (\mu_1 \mu_2 k_1 k_2) \Gamma_5 + (\mathbf{k}_1 \cdot \mathbf{k}_2) \Gamma_6 + (k_1^2 + k_2^2) \Gamma_7 + (\mu_1^2 k_1^2 + \mu_2^2 k_2^2) \Gamma_8 \\ &+ i \left[(\mu_1 k_1^3 + \mu_2 k_2^3) \Gamma_9 + (\mu_1 k_1 + \mu_2 k_2) (\mathbf{k}_1 \cdot \mathbf{k}_2) \Gamma_{10} + k_1 k_2 (\mu_1 k_2 + \mu_2 k_1) \Gamma_{11} \right. \\ &\left. \left. + (\mu_1^3 k_1^3 + \mu_2^3 k_2^3) \Gamma_{12} + \mu_1 \mu_2 k_1 k_2 (\mu_1 k_1 + \mu_2 k_2) \Gamma_{13} + \mu_3 \frac{k_1^2 k_2^2}{k_3} G_2(\mathbf{k}_1, \mathbf{k}_2) \Gamma_{14} \right] \right\}, \end{aligned} \quad (55)$$

where the $\Gamma_I(z)$ are given in Appendix C.

We have ordered the Γ_I according to the powers of \mathcal{H}/k , starting with the $\mathcal{O}(\mathcal{H}^4/k^4)$ term and ending with the $\mathcal{O}(\mathcal{H}/k)$ terms. This is our key result – transforming the highly complicated second-order GR projection corrections given by (31) into a manageable Fourier-space kernel (55). In the special case $b_e = 0 = \mathcal{Q}$, (31) reduces to the form given in [28]. When b_e, \mathcal{Q} are nonzero, the Γ_I become much more complicated.

In Fourier space, the observed galaxy bispectrum B_g at fixed redshift is given by

$$\langle \Delta_g(\mathbf{k}_1) \Delta_g(\mathbf{k}_2) \Delta_g(\mathbf{k}_3) \rangle = (2\pi)^3 B_g(\mathbf{k}_1, \mathbf{k}_2, \mathbf{k}_3) \delta^D(\mathbf{k}_1 + \mathbf{k}_2 + \mathbf{k}_3). \quad (56)$$

At second order, the only combinations of terms that contribute at tree-level are

$$\begin{aligned} 2\langle \Delta_g(\mathbf{k}_1) \Delta_g(\mathbf{k}_2) \Delta_g(\mathbf{k}_3) \rangle &= \langle \Delta_g^{(1)}(\mathbf{k}_1) \Delta_g^{(1)}(\mathbf{k}_2) \Delta_g^{(2)}(\mathbf{k}_3) \rangle + 2 \text{cyc. perm.} \\ &= \langle \Delta_{gN}^{(1)}(\mathbf{k}_1) \Delta_{gN}^{(1)}(\mathbf{k}_2) \Delta_{gN}^{(2)}(\mathbf{k}_3) \rangle + \langle \Delta_{g\text{GR}}^{(1)}(\mathbf{k}_1) \Delta_{g\text{GR}}^{(1)}(\mathbf{k}_2) \Delta_{g\text{GR}}^{(2)}(\mathbf{k}_3) \rangle \\ &+ \langle \Delta_{gN}^{(1)}(\mathbf{k}_1) \Delta_{gN}^{(1)}(\mathbf{k}_2) \Delta_{g\text{GR}}^{(2)}(\mathbf{k}_3) \rangle + \langle \Delta_{g\text{GR}}^{(1)}(\mathbf{k}_1) \Delta_{g\text{GR}}^{(1)}(\mathbf{k}_2) \Delta_{gN}^{(2)}(\mathbf{k}_3) \rangle \\ &+ 2 \left[\langle \Delta_{gN}^{(1)}(\mathbf{k}_1) \Delta_{g\text{GR}}^{(1)}(\mathbf{k}_2) \Delta_{gN}^{(2)}(\mathbf{k}_3) \rangle + \langle \Delta_{gN}^{(1)}(\mathbf{k}_1) \Delta_{g\text{GR}}^{(1)}(\mathbf{k}_2) \Delta_{g\text{GR}}^{(2)}(\mathbf{k}_3) \rangle \right] \\ &+ 2 \text{cyc. perm.}, \end{aligned} \quad (57)$$

where the factors of 2 arise from the factor 1/2 in the perturbative expansion of Δ_g . In the second equality, we have further separated the bispectrum into purely Newtonian and purely GR parts (first line), and cross-correlations between Newtonian and GR terms (following lines). The cross-correlation terms become important on smaller scales than the pure GR term.

The full expression for the galaxy bispectrum in terms of kernels follows from (58) as:

$$\begin{aligned} B_g(\mathbf{k}_1, \mathbf{k}_2, \mathbf{k}_3) &= \left[\mathcal{K}_N^{(1)}(\mathbf{k}_1) \mathcal{K}_N^{(1)}(\mathbf{k}_2) \mathcal{K}_N^{(2)}(\mathbf{k}_1, \mathbf{k}_2, \mathbf{k}_3) + \mathcal{K}_{\text{GR}}^{(1)}(\mathbf{k}_1) \mathcal{K}_{\text{GR}}^{(1)}(\mathbf{k}_2) \mathcal{K}_{\text{GR}}^{(2)}(\mathbf{k}_1, \mathbf{k}_2, \mathbf{k}_3) \right. \\ &+ \mathcal{K}_N^{(1)}(\mathbf{k}_1) \mathcal{K}_N^{(1)}(\mathbf{k}_2) \mathcal{K}_{\text{GR}}^{(2)}(\mathbf{k}_1, \mathbf{k}_2, \mathbf{k}_3) + \mathcal{K}_{\text{GR}}^{(1)}(\mathbf{k}_1) \mathcal{K}_{\text{GR}}^{(1)}(\mathbf{k}_2) \mathcal{K}_N^{(2)}(\mathbf{k}_1, \mathbf{k}_2, \mathbf{k}_3) \\ &\left. + 2\mathcal{K}_N^{(1)}(\mathbf{k}_1) \mathcal{K}_{\text{GR}}^{(1)}(\mathbf{k}_2) \left\{ \mathcal{K}_N^{(2)}(\mathbf{k}_1, \mathbf{k}_2, \mathbf{k}_3) + \mathcal{K}_{\text{GR}}^{(2)}(\mathbf{k}_1, \mathbf{k}_2, \mathbf{k}_3) \right\} \right] P(k_1) P(k_2) + 2 \text{cyc. perm.} \end{aligned} \quad (59)$$

The bispectrum in the Newtonian approximation is

$$B_{gN}(\mathbf{k}_1, \mathbf{k}_2, \mathbf{k}_3) = \mathcal{K}_N^{(1)}(\mathbf{k}_1)\mathcal{K}_N^{(1)}(\mathbf{k}_2)\mathcal{K}_N^{(2)}(\mathbf{k}_1, \mathbf{k}_2, \mathbf{k}_3)P(k_1)P(k_2) + 2 \text{ cyc. perm.} \quad (60)$$

All other terms in (59) are GR corrections, i.e., they vanish if the GR projection effects are neglected.

Calculation of the galaxy bispectrum including all the GR terms leads to a complex-valued function. We split (59) into real and imaginary parts $B_g = B_g^R + iB_g^I$ and compute the absolute value of the galaxy bispectrum, given by $|B_g|^2 = (B_g^R)^2 + (B_g^I)^2$.

There are four different angles implicit in (59):

- three θ_i between the observer line of sight and the mode vectors (with cosines $\mu_i = \cos \theta_i = \hat{\mathbf{k}}_i \cdot \mathbf{n}$)
- + one of the angles θ_{ij} between \mathbf{k}_i and \mathbf{k}_j (with cosines $\mu_{ij} = \cos \theta_{ij} = \hat{\mathbf{k}}_i \cdot \hat{\mathbf{k}}_j$).

Two of the μ_i are independent, since $\mu_1 k_1 + \mu_2 k_2 + \mu_3 k_3 = 0$, where $k_3 = |\mathbf{k}_1 + \mathbf{k}_2|$. Two of the μ_{ij} can be determined by the third via trigonometric identities. Finally, one of the two remaining μ_i may be expressed in terms of the other one and the choice of independent μ_{ij} , using the trigonometric addition formula. If we choose μ_1 and μ_{12} , then

$$\mu_2 = \mu_1 \mu_{12} \pm \sqrt{1 - \mu_1^2} \sqrt{1 - \mu_{12}^2} \cos \phi, \quad (61)$$

where μ_{12} can be determined from the k_i . Here ϕ is the azimuthal angle, characterizing the orientation of the triangle in Fourier space, and the \pm arises due to invariance under reflection of \mathbf{n} about $\hat{\mathbf{k}}_2$ in their plane.

Implementing these conditions, the galaxy bispectrum is a function of μ_1 and ϕ , together with the magnitudes of the three mode vectors. The dependence of B_g on μ_1 and ϕ may be expanded in spherical harmonics:

$$B_g(k_1, k_2, k_3, \mu_1, \phi) = \sum_{\ell=0}^{\infty} \sum_{m=-\ell}^{\ell} B_g^{\ell m}(k_1, k_2, k_3) Y_{\ell m}(\mu_1, \phi), \quad (62)$$

where the multipoles of B_g are given by

$$B_g^{\ell m}(k_1, k_2, k_3) = \frac{(2\ell + 1)}{4\pi} \int_0^{2\pi} d\phi \int_{-1}^1 d\mu_1 B_g(k_1, k_2, k_3, \mu_1, \phi) Y_{\ell m}^*(\mu_1, \phi). \quad (63)$$

This can be compared to the Legendre multipole expansion of the galaxy power spectrum

$$P_g(k, \mu) = \sum_{\ell=0}^{\ell_{\max}} P_g^{\ell}(k) \mathcal{L}_{\ell}(\mu) \quad \text{with} \quad P_g^{\ell}(k) = \frac{(2\ell + 1)}{2} \int_{-1}^1 d\mu P_g(k, \mu) \mathcal{L}_{\ell}(\mu). \quad (64)$$

Note that we can also expand the bispectrum in Associated Legendre polynomials and still recover the multipoles as given in (63).

Typically, only the $m = 0$ multipoles of B_g are considered, and we will do this, so that $B_g = B_g(k_1, k_2, k_3, \mu_1)$. In fact, this does not lose much information [52]. For the monopole, we use the shorthand $B_g^0 \equiv B_g^{00}$.

IV. NUMERICAL RESULTS

In order to illustrate quantitatively the imprint of GR effects on the galaxy bispectrum, we specialise to an isosceles configuration, with

$$k_1 = k_2 \equiv k, \quad k_3 = k\sqrt{2(1 + \mu_{12})}. \quad (65)$$

We evaluate the following cases:

$$\text{radial: } \mu_1 = 1 \rightarrow B_g^{\parallel}, \quad \text{transverse: } \mu_1 = 0 \rightarrow B_g^{\perp}, \quad \text{monopole: } \int d\mu_1 \rightarrow B_g^0. \quad (66)$$

For redshifts and astrophysical parameters, we choose:

$$z = 1.0, 1.5, \quad b_1(z) = \sqrt{1+z}, \quad b_2(z) = -0.1\sqrt{1+z}, \quad b_e = 0 = \mathcal{Q}, \quad (67)$$

where the galaxy bias parameters are similar to [53].

In each case, we compare the Newtonian prediction (60) for the galaxy bispectrum, to the GR prediction (59). We consider the galaxy bispectrum B_g as a function of triangle size for two isosceles shapes. We fix $\mu_{12} = \cos\theta_{12}$ and vary k , for two special cases:

$$\text{equilateral: } \mu_{12} = -\frac{1}{2}, \quad \text{moderately squeezed: } \mu_{12} = -0.998 \Rightarrow k_3 \approx \frac{k}{16}. \quad (68)$$

Figure 1 shows the radial, transverse and monopole parts of B_g , together with the percentage correction relative to the Newtonian case without the GR projection effects, on scales $0.01 \leq k \leq 0.1$, which includes BAO scales. In all cases, as expected, the GR corrections become increasingly important on larger scales. The squeezed configuration has a larger correction than the equilateral. For the monopole, the GR correction at equality scales reaches $\mathcal{O}(30 - 70\%)$ at $z \sim 1 - 1.5$, and then grows larger. Note that when the short modes are equality scale, the long mode is still within the Hubble horizon:

$$k \sim k_{\text{eq}} \Rightarrow k_3 \sim \frac{k_{\text{eq}}}{16} \sim 3H_0. \quad (69)$$

On the largest scales, our results need to be corrected for wide-angle correlations that are absent in the plane-parallel approximation.

It is interesting to identify the various contributions to the galaxy bispectrum monopole in Fig. 1. We do this in two ways, as illustrated in Fig. 2, for the moderately squeezed (left) and equilateral (right) shapes, at $z = 1.5$:

- In the top panel, we show the contributions from the various 3-point correlations $\langle \Delta_g(\mathbf{k}_1)\Delta_g(\mathbf{k}_2)\Delta_g(\mathbf{k}_3) \rangle$, as given in (58).

The pure Newtonian correlation gives the standard curve (dashed, black). The 5 solid curves are the correlations with GR corrections: 1 pure GR correlation (red), which dominates on horizon scales, and 4 correlations between GR and Newtonian. It can be seen that 3 of the mixed correlation terms (blue, green, magenta) dominate the GR correction on subhorizon scales.

For the squeezed case, the dominant correlation is $\langle \Delta_{gN}^{(1)}(\mathbf{k}_1)\Delta_{gGR}^{(1)}(\mathbf{k}_2)\Delta_{gGR}^{(2)}(\mathbf{k}_3) \rangle$ (blue). If we omitted the second-order GR projection effects, we would miss this dominant GR contribution to the squeezed galaxy bispectrum.

Note that the correlation with only one GR first-order projection term, i.e., $\langle \Delta_{gN}^{(1)}(\mathbf{k}_1)\Delta_{gGR}^{(1)}(\mathbf{k}_2)\Delta_{gN}^{(2)}(\mathbf{k}_3) \rangle$ (magenta), has a constant contribution on super-equality scales.

- In the bottom panel, we show the contributions from the first-order GR kernel $\mathcal{K}_{GR}^{(1)}$, (51), on its own (red), and then together with the terms in the second-order GR kernel $\mathcal{K}_{GR}^{(2)}$, (55), split into powers of k^{-1} .

The first-order GR correction (red) clearly under-estimates the full GR correction, especially in the squeezed case.

Amongst the second-order GR corrections in the squeezed case, the k^{-1} term (blue) dominates on ultra-large scales until close to the comoving horizon, $k = \mathcal{H}$, when the k^{-n} , $n = 2, 3, 4$ terms (green, magenta, orange) dominate.

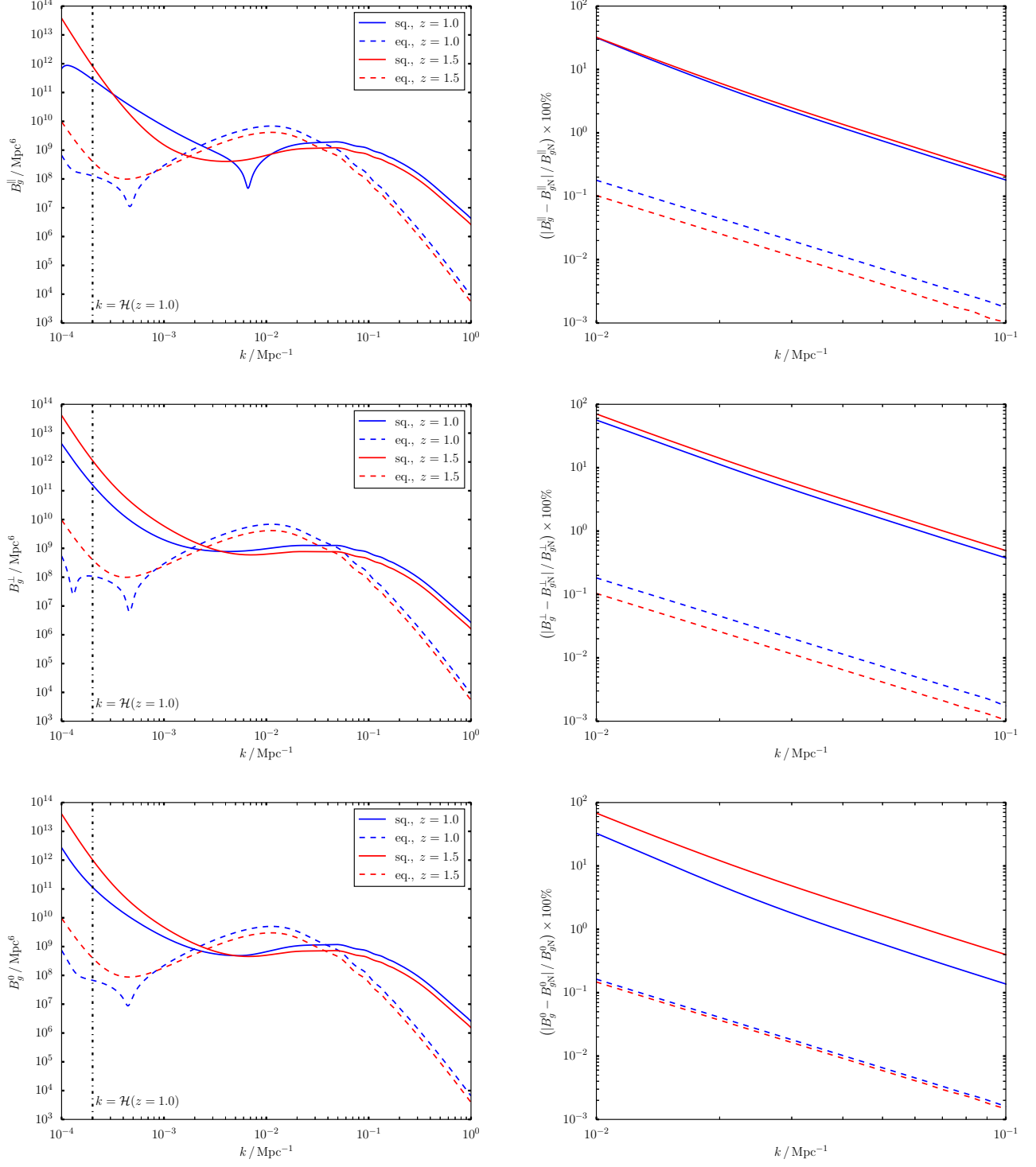


FIG. 1. *Left:* Galaxy bispectrum for moderately squeezed ($k_3 \approx k/16$, solid) and equilateral ($k_3 = k$, dashed) shapes, at $z = 1.0, 1.5$. From top to bottom: radial, transverse and monopole parts. *Right:* Percentage difference relative to the Newtonian approximation for $0.01 \leq k \leq 0.1$, which includes BAO scales.

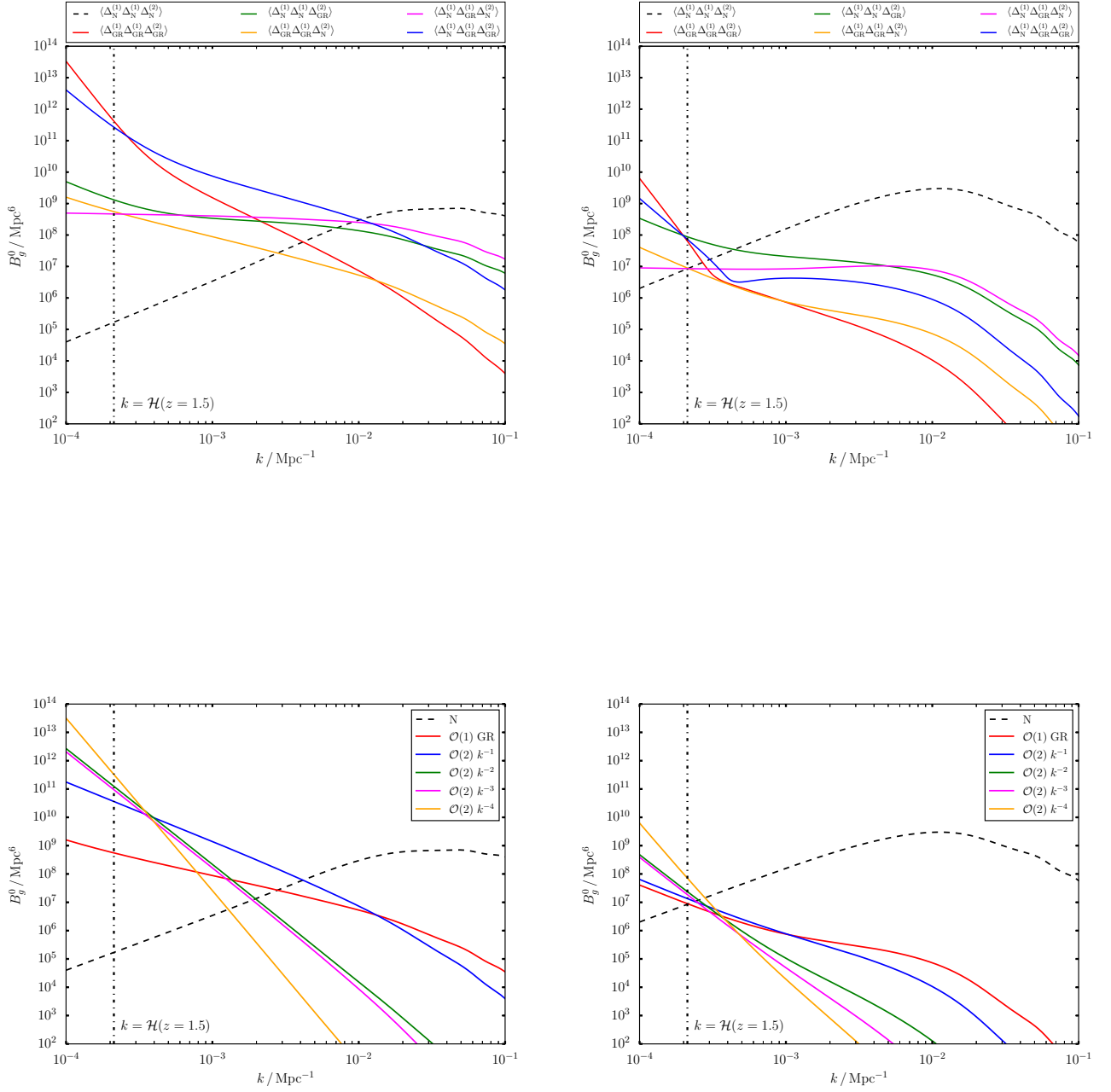


FIG. 2. Contributions to the galaxy bispectrum monopole for the moderately squeezed (*left*) and equilateral (*right*) shapes of Fig. 1, at $z = 1.5$.

Top: The different 3-point correlations that contribute to the galaxy bispectrum – purely Newtonian, purely GR and mixed correlations – as given in (58).

Bottom: The different contributions to the galaxy bispectrum from the first order GR kernel (51) on its own, and then together with the terms in the second order GR kernel (55), split into powers of k^{-1} .

On scales around equality, we can find a power-law fit for the fractional GR corrections to the Newtonian prediction:

$$B_g^{(s)} = B_{gN}^{(s)} \left[1 + \Delta B^{(s)} \right] \quad s = \text{radial, transverse, monopole}, \quad (70)$$

$$\Delta B^{(s)} = \alpha^{(s)} \left(\frac{k}{k_{\text{eq}}} \right)^{-n} \quad 0.007 \text{ Mpc}^{-1} \lesssim k \lesssim 0.07 \text{ Mpc}^{-1}. \quad (71)$$

We find that $n = 2$ is a good fit for all s and redshift, and for squeezed and equilateral cases. This shows that the dominant GR corrections add up to behave as $\mathcal{O}(\mathcal{H}^2/k^2)$ around equality scales. The amplitude on equality scales, $\alpha^{(s)}$, varies weakly with s and z , but is significantly smaller for equilateral shapes – see Table I.

	$\alpha^{(s)} \times 10^2$ for $z = 1, 1.5$	Triangle shape
ΔB^{\parallel}	32.8, 32.2 .17, .096	squeezed equilateral
ΔB^{\perp}	54.1, 69.6 .17, .096	squeezed equilateral
ΔB^0	33.5, 69.4 .15, .14	squeezed equilateral

TABLE I. Percentage GR corrections at equality, as defined in (71), for the bispectra in Fig. 1.

V. CONCLUSION

We considered the local relativistic projection effects on the galaxy bispectrum, up to second order, providing the details behind the results presented in [28], and generalizing those results to include evolution bias and magnification bias. We transformed the local GR contribution into Fourier space, to form the kernel $\mathcal{K}_{\text{GR}}^{(2)}(\mathbf{k}_1, \mathbf{k}_2, \mathbf{k}_3)$ given by (55), with further details presented in Appendix B, and the Γ_I coefficients given in Appendix C. Once we have this kernel, computing the bispectrum is a relatively straightforward procedure, which allows us to analyse the contribution from GR effects to the bispectrum.

We incorporated a careful treatment of galaxy bias on ultra-large scales, which is essential in order to avoid spurious gauge effects. We assumed a simple local-in-mass-density model of nonlinear bias that neglects tidal effects, leading to the relativistic bias relation (26) for the Poisson-gauge galaxy number density contrast.

The GR effects can be significant, as illustrated in Fig. 1 and Table I, for equilateral and moderately squeezed triangles in the radial, transverse and monopole parts of the bispectrum. On equality scales at $z \sim 1 - 1.5$ they alter the bispectrum monopole in the moderately squeezed case by $\sim 30 - 70\%$. On ultra-large scales, the bispectrum is dominated by the local GR terms.

The contributions to the total GR correction of the monopole are shown in Fig. 2. The top panel presents the contributions from the various 3-point correlations given in (58). In the squeezed case, the dominant correlation is

$$\langle \Delta_{gN}^{(1)}(\mathbf{k}_1) \Delta_{g\text{GR}}^{(1)}(\mathbf{k}_2) \Delta_{g\text{GR}}^{(2)}(\mathbf{k}_3) \rangle.$$

If we included only the first-order GR projection effects in our analysis, we would miss this dominant GR contribution to the squeezed galaxy bispectrum. The bottom panel breaks down the terms in the second-order GR kernel $\mathcal{K}_{\text{GR}}^{(2)}$ according to powers of k^{-1} . For the squeezed case, the k^{-1} term dominates on ultra-large scales until close to the comoving horizon, $k = \mathcal{H}$.

Our main aim was to highlight the importance of the effects from observations, properly analysed in GR, and to this end, we treated the simplest case, taking the first steps towards a complete analysis. We have not included:

- primordial non-Gaussianity;
- tidal stress in the galaxy bias;
- GR corrections to the $v^{(2)}$, $\Phi^{(2)}$ and $\Psi^{(2)}$ terms that contribute to the projection effects;
- the second-order effect of the radiation era on initial conditions for sub-equality modes;
- integrated contributions to the projection effects, wide-angle correlations and radial (cross-bin) correlations.

The first three effects can be incorporated within our Fourier-space analysis using the plane-parallel approximation. The fourth requires numerical integration with a second-order Boltzmann code [35]. The last requires one to use the 3-point correlation function, for example through a spherical harmonic decomposition.⁵

Acknowledgments:

We are especially grateful to Kazuya Koyama for very helpful comments. We thank Tobias Baldauf, Daniele Bertacca, Ruth Durrer, Sabino Matarrese and David Wands for useful discussions and comments. We also thank an anonymous referee for very useful comments. All authors are funded in part by the NRF (South Africa). OU, SJ and RM are also supported by the South African SKA Project. RM and CC are also supported by the UK STFC, Grants ST/N000668/1 (RM) and ST/P000592/1 (CC).

⁵ After our paper was completed, [54] presented a formalism for analysing the 3-point correlation function with all GR effects included, but without computation of the effects.

Appendix A: Second-order gauge transformation of number density contrast

At second order, the number density contrasts in Poisson and C gauges are related by a generalisation of (17), which is given in [30]:

$$\begin{aligned}
\delta_g^{(2)} &= \delta_{gC}^{(2)} + (3 - b_e)\mathcal{H}v^{(2)} + \left[(b_e - 3)\mathcal{H}' + b'_e\mathcal{H} + (b_e - 3)^2\mathcal{H}^2 \right] [v^{(1)}]^2 + (b_e - 3)\mathcal{H}v^{(1)}v^{(1)'} \\
&\quad - (b_e - 3)\mathcal{H}\nabla^{-2} \left[v^{(1)}\nabla^2 v^{(1)'} - v^{(1)'}\nabla^2 v^{(1)} - 6\partial_i\Phi^{(1)}\partial^i v^{(1)} - 6\Phi^{(1)}\nabla^2 v^{(1)} \right] + 2(3 - b_e)\mathcal{H}v^{(1)}\delta_{gC}^{(1)} - 2v^{(1)}\delta_{gC}^{(1)'} \\
&\quad - \frac{1}{2}\partial^i\xi^{(1)} \left[(3 - b_e)\mathcal{H}\partial_i v^{(1)} + 2\partial_i\delta_{gC}^{(1)} \right] \\
&\quad - \frac{1}{2}(b_e - 3)\mathcal{H}\nabla^{-2} \left[\partial_i\xi^{(1)}\partial^i\nabla^2 v^{(1)} + \partial_i v^{(1)}\partial^i\nabla^2\xi^{(1)} + 2\partial_i\partial_j\xi^{(1)}\partial^i\partial^j v^{(1)} \right]. \tag{A1}
\end{aligned}$$

Here $\xi^{(1)}$ is a gauge generator, and the residual C-gauge freedom is fixed by imposing $\xi^{(1)'} = 2v^{(1)}$ [30].

It follows from the identity

$$\nabla^2 \left[\partial_i\xi^{(1)} \cdot \partial^i v^{(1)} \right] = \partial^i v^{(1)} \cdot \nabla^2 \left[\partial_i\xi^{(1)} \right] + \partial_i\xi^{(1)} \cdot \nabla^2 \left[\partial^i v^{(1)} \right] + 2\partial_j\partial_i\xi^{(1)} \cdot \partial^j\partial^i v^{(1)}, \tag{A2}$$

that the last line of (A1) reduces to $-(b_e - 3)\mathcal{H}\partial_i\xi^{(1)}\partial^i v^{(1)}/2$, which cancels the first term on the third line. Thus (A1) may be simplified to

$$\begin{aligned}
\delta_g^{(2)} &= \delta_{gC}^{(2)} + (3 - b_e)\mathcal{H}v^{(2)} + \left[(b_e - 3)\mathcal{H}' + b'_e\mathcal{H} + (b_e - 3)^2\mathcal{H}^2 \right] [v^{(1)}]^2 + (b_e - 3)\mathcal{H}v^{(1)}v^{(1)'} \\
&\quad - (b_e - 3)\mathcal{H}\nabla^{-2} \left[v^{(1)}\nabla^2 v^{(1)'} - v^{(1)'}\nabla^2 v^{(1)} - 6\partial_i\Phi^{(1)}\partial^i v^{(1)} - 6\Phi^{(1)}\nabla^2 v^{(1)} \right] + 2(3 - b_e)\mathcal{H}v^{(1)}\delta_{gC}^{(1)} - 2v^{(1)}\delta_{gC}^{(1)'} \\
&\quad - \left[\partial_i\delta_{gC}^{(1)} \right] \partial^i\xi^{(1)}. \tag{A3}
\end{aligned}$$

By the continuity equation, given in (13), the gauge fixing condition $\xi^{(1)'} = 2v^{(1)}$ implies that

$$\partial^i\xi^{(1)} = -2\nabla^{-2}\partial^i\delta_{mC}^{(1)}. \tag{A4}$$

Using this, the relation (22) between C- and T-gauge number density contrasts becomes

$$\delta_{gC}^{(2)} - \left[\partial_i\delta_{gC}^{(1)} \right] \partial^i\xi^{(1)} = \delta_{gT}^{(2)}. \tag{A5}$$

Then it follows from (A3) and (A5) that (A1) can be rewritten as the second-order map from the Poisson-gauge δ_g to the T-gauge δ_{gT} :

$$\begin{aligned}
\delta_g^{(2)} &= \delta_{gT}^{(2)} + (3 - b_e)\mathcal{H}v^{(2)} + \left[(b_e - 3)\mathcal{H}' + b'_e\mathcal{H} + (b_e - 3)^2\mathcal{H}^2 \right] [v^{(1)}]^2 + (b_e - 3)\mathcal{H}v^{(1)}v^{(1)'} \\
&\quad - (b_e - 3)\mathcal{H}\nabla^{-2} \left[v^{(1)}\nabla^2 v^{(1)'} - v^{(1)'}\nabla^2 v^{(1)} - 6\partial_i\Phi^{(1)}\partial^i v^{(1)} - 6\Phi^{(1)}\nabla^2 v^{(1)} \right] \\
&\quad + 2(3 - b_e)\mathcal{H}v^{(1)}\delta_{gT}^{(1)} - 2v^{(1)}\delta_{gT}^{(1)'}. \tag{A6}
\end{aligned}$$

This is (25).

Appendix B: Expansion of perturbed variables in Fourier space

We express all variables in terms of the T-gauge matter density contrast, $\delta(\mathbf{k})$. For the gravitational and velocity potentials, (14), (15) and (18) give

$$\mathcal{H}v^{(1)}(\mathbf{k}) = f\frac{\mathcal{H}^2}{k^2}\delta^{(1)}(\mathbf{k}), \quad \Phi^{(1)}(\mathbf{k}) = -\frac{3}{2}\Omega_m\frac{\mathcal{H}^2}{k^2}\delta^{(1)}(\mathbf{k}). \quad (\text{B1})$$

The growth rate and growth suppression factor in Λ CDM obey

$$\frac{f'}{\mathcal{H}} = \frac{1}{2}(3\Omega_m - 4)f - f^2 + \frac{3}{2}\Omega_m, \quad \frac{1}{\mathcal{H}}\frac{g'}{g} = f - 1. \quad (\text{B2})$$

The galaxy number density contrast in Fourier space is expanded using (16), (17):

$$\delta_g^{(1)} = b_1\delta^{(1)} + (3 - b_e)\mathcal{H}v^{(1)}. \quad (\text{B3})$$

The evolution of the velocity potential follows from the Euler equation as

$$v^{(1)'} = -\mathcal{H}v^{(1)} - \Phi^{(1)}. \quad (\text{B4})$$

The time derivative of the galaxy number density contrast follows from (B3) and (B4) as

$$\delta_g^{(1)'} = (b_1' + b_1f\mathcal{H})\delta^{(1)} + [(3 - b_e)(\mathcal{H}' - \mathcal{H}^2) - b_e'\mathcal{H}]v^{(1)} - (3 - b_e)\mathcal{H}\Phi^{(1)}. \quad (\text{B5})$$

At second order, a typical term such as $v^{(1)}(\mathbf{x})\delta_g^{(1)}(\mathbf{x})$ can be expressed as:

$$\begin{aligned} v^{(1)}(\mathbf{x})\delta_g^{(1)}(\mathbf{x}) &= \int \frac{d^3k}{(2\pi)^3} e^{i\mathbf{k}\cdot\mathbf{x}} [v^{(1)}\delta_g^{(1)}](\mathbf{k}), \quad (\text{B6}) \\ [v^{(1)}\delta_g^{(1)}](\mathbf{k}) &= \int d^3x e^{-i\mathbf{k}\cdot\mathbf{x}} v^{(1)}(\mathbf{x})\delta_g^{(1)}(\mathbf{x}) \\ &= \frac{1}{2} \int d^3x \int \frac{d^3k_1}{(2\pi)^3} \frac{d^3k_2}{(2\pi)^3} [v^{(1)}(\mathbf{k}_1)\delta_g^{(1)}(\mathbf{k}_2) + v^{(1)}(\mathbf{k}_2)\delta_g^{(1)}(\mathbf{k}_1)] e^{-i\mathbf{k}\cdot\mathbf{x}} e^{i\mathbf{k}_1\cdot\mathbf{x}} e^{i\mathbf{k}_2\cdot\mathbf{x}} \\ &= \frac{1}{2} \int \frac{d^3k_1}{(2\pi)^3} \frac{d^3k_2}{(2\pi)^3} [v^{(1)}(\mathbf{k}_1)\delta_g^{(1)}(\mathbf{k}_2) + v^{(1)}(\mathbf{k}_2)\delta_g^{(1)}(\mathbf{k}_1)] (2\pi)^3 \delta^D(\mathbf{k}_1 + \mathbf{k}_2 - \mathbf{k}), \quad (\text{B7}) \end{aligned}$$

where we used (39) and the definition of the Dirac delta function in three dimensions. Then we express the perturbative variables in terms of $\delta^{(1)}$, using (B1) and (B3):

$$v^{(1)}(\mathbf{k}_1)\delta_g^{(1)}(\mathbf{k}_2) + v^{(1)}(\mathbf{k}_2)\delta_g^{(1)}(\mathbf{k}_1) = \left[b_1f\mathcal{H}\left(\frac{1}{k_1^2} + \frac{1}{k_2^2}\right) + 2f^2(3 - b_e)\mathcal{H}^3\frac{1}{k_1^2k_2^2} \right] \delta^{(1)}(\mathbf{k}_1)\delta^{(1)}(\mathbf{k}_2). \quad (\text{B8})$$

This leads to

$$[v^{(1)}\delta_g^{(1)}](\mathbf{k}) = \int \frac{d^3k_1}{(2\pi)^3} \frac{d^3k_2}{(2\pi)^3} \mathcal{F}[v^{(1)}\delta_g^{(1)}] \delta^{(1)}(\mathbf{k}_1)\delta^{(1)}(\mathbf{k}_2)(2\pi)^3 \delta^D(\mathbf{k}_1 + \mathbf{k}_2 - \mathbf{k}), \quad (\text{B9})$$

where the kernel is

$$\mathcal{F}[v^{(1)}(\mathbf{x})\delta_g^{(1)}(\mathbf{x})] = f\mathcal{H} \frac{[b_1(k_1^2 + k_2^2) + 2(3 - b_e)f\mathcal{H}^2]}{2k_1^2k_2^2}. \quad (\text{B10})$$

Table II gives the Fourier kernels for all second-order terms in $\Delta_g^{(2)}$.

TABLE II. Fourier transform kernel and coefficient of each term of (30) and (31), ordered according to their k -dependence. N denotes a Newtonian term (k^0), Γ_1 is for k^{-4} , Γ_2 is for k^{-3} , Γ_3 to Γ_8 are for k^{-2} and Γ_9 to Γ_{14} are for k^{-1} . For convenience, the superscript (1) is dropped from first-order variables $\delta^{(1)}$, $v^{(1)}$, $\Phi^{(1)}$.

Term	Γ	Fourier kernel \mathcal{F}	Coefficient
$\delta^{(2)}$	N	$F_2(\mathbf{k}_1, \mathbf{k}_2)$	b_1
$\partial_{\parallel}^2 v^{(2)}$	N	$f^2 \mathcal{H} \mu_3^2 G_2(\mathbf{k}_1, \mathbf{k}_2)$	$-1/\mathcal{H}$
$\delta \partial_{\parallel}^2 v$	N	$-f \mathcal{H} (\mu_1^2 + \mu_2^2)/2$	$-2b_1/\mathcal{H}$
$\partial_{\parallel} v \partial_{\parallel} \delta$	N	$-f \mathcal{H} \mu_1 \mu_2 (k_1^2 + k_2^2)/(2k_1 k_2)$	$-2b_1/\mathcal{H}$
$\partial_{\parallel} v \partial_{\parallel}^3 v$	N	$f^2 \mathcal{H}^2 (\mu_1 \mu_2^3 k_2^2 + \mu_2 \mu_1^3 k_1^2)/(k_1 k_2)$	$2/\mathcal{H}^2$
$[\partial_{\parallel}^2 v]^2$	N	$f^2 \mathcal{H}^2 \mu_1^2 \mu_2^2$	$2/\mathcal{H}^2$
$[\Phi]^2$	Γ_1	$9\Omega_m^2 \mathcal{H}^4/(4k_1^2 k_2^2)$	\mathcal{A}
Φv	Γ_1	$-3\Omega_m \mathcal{H}^3 f/(2k_1^2 k_2^2)$	\mathcal{C}
$\nabla^{-2}(v \nabla^2 v' - v' \nabla^2 v - 6\partial_i \Phi \partial^i v - 6\Phi \nabla^2 v)$	Γ_1	$9\Omega_m \mathcal{H}^3 f/(2k_1^2 k_2^2)$	$(3 - b_e)\mathcal{H}$
vv'	Γ_1	$f \mathcal{H}^3 (3\Omega_m - 2f)/(2k_1^2 k_2^2)$	$(b_e - 3)\mathcal{H}$
$[v]^2$	Γ_1	$f^2 \mathcal{H}^2/(k_1^2 k_2^2)$	$(b_e - 3)^2 \mathcal{H}^2 + b_e' \mathcal{H} + (b_e - 3)\mathcal{H}'$
$v \partial_{\parallel} v$	Γ_2	$i f^2 \mathcal{H}^2 (\mu_1 k_1 + \mu_2 k_2)/(2k_1^2 k_2^2)$	\mathcal{B}
$\Phi \partial_{\parallel} v$	Γ_2	$-3i f \Omega_m \mathcal{H}^3 (\mu_1 k_1 + \mu_2 k_2)/(4k_1^2 k_2^2)$	\mathcal{D}
$\Phi \partial_{\parallel} \Phi$	Γ_2	$9i \Omega_m^2 \mathcal{H}^4 (\mu_1 k_1 + \mu_2 k_2)/(8k_1^2 k_2^2)$	$2(f - 2 + 2\mathcal{Q})/\mathcal{H}$
$\Psi^{(2)} = \Phi^{(2)}$	Γ_3	$-3\Omega_m \mathcal{H}^2 F_2(\mathbf{k}_1, \mathbf{k}_2)/(2k_3^2)$	$4\mathcal{Q} - 1 - b_e + R$
$\Phi^{(2)'}$	Γ_3	$-3\Omega_m \mathcal{H}^3 (2f - 1) F_2(\mathbf{k}_1, \mathbf{k}_2)/(2k_3^2)$	$1/\mathcal{H}$
$v^{(2)}$	Γ_4	$f \mathcal{H} G_2(\mathbf{k}_1, \mathbf{k}_2)/k_3^2$	$(3 - b_e)\mathcal{H}$
$[\partial_{\parallel} v]^2$	Γ_5	$-f^2 \mathcal{H}^2 \mu_1 \mu_2/(k_1 k_2)$	\mathcal{E}
$\partial_{\parallel} v \partial_{\parallel} \Phi$	Γ_5	$3f \Omega_m \mathcal{H}^3 \mu_1 \mu_2/(2k_1 k_2)$	$2(2 - f - 2\mathcal{Q})/\mathcal{H}$
$\partial_i v \partial^i v$	Γ_6	$-f^2 \mathcal{H}^2 \mathbf{k}_1 \cdot \mathbf{k}_2/(k_1^2 k_2^2)$	$b_e - 1 - 2\mathcal{Q} - R$
$\partial_i v \partial^i \Phi$	Γ_6	$3f \Omega_m \mathcal{H}^3 \mathbf{k}_1 \cdot \mathbf{k}_2/(2k_1^2 k_2^2)$	$2/\mathcal{H}$

$\Phi\delta$	Γ_7	$-3\Omega_m\mathcal{H}^2(k_1^2+k_2^2)/(4k_1^2k_2^2)$	$2b_1(f-2-b_e+4\mathcal{Q}+R)-S$
$\Phi\delta'$	Γ_7	$-3f\Omega_m\mathcal{H}^3(k_1^2+k_2^2)/(4k_1^2k_2^2)$	$-2b_1/\mathcal{H}$
$v\delta$	Γ_7	$f\mathcal{H}(k_1^2+k_2^2)/(2k_1^2k_2^2)$	$b'_1+2b_1(3-b_e)\mathcal{H}$
$v\delta'$	Γ_7	$f^2\mathcal{H}^2(k_1^2+k_2^2)/(2k_1^2k_2^2)$	$-2b_1$
$\Phi\partial_{\parallel}^2v$	Γ_8	$3f\Omega_m\mathcal{H}^3(\mu_1^2k_1^2+\mu_2^2k_2^2)/(4k_1^2k_2^2)$	$2(1-2f+2b_e-6\mathcal{Q}-2R-\mathcal{H}'/\mathcal{H}^2)/\mathcal{H}$
$\Phi\partial_{\parallel}^2\Phi$	Γ_8	$-9\Omega_m^2\mathcal{H}^4(\mu_1^2k_1^2+\mu_2^2k_2^2)/(4k_1^2k_2^2)$	$-2/\mathcal{H}^2$
$v\partial_{\parallel}^2v$	Γ_8	$-f^2\mathcal{H}^3(\mu_1^2k_1^2+\mu_2^2k_2^2)/(2k_1^2k_2^2)$	$2(b_e-3)/\mathcal{H}$
$\Phi\partial_{\parallel}\delta$	Γ_9	$-3i\Omega_m\mathcal{H}^2(\mu_1k_1^3+\mu_2k_2^3)/(4k_1^2k_2^2)$	$2b_1/\mathcal{H}$
$\partial_i v \partial_{\parallel} \partial^i v$	Γ_{10}	$-i f^2 \mathcal{H}^2 \mathbf{k}_1 \cdot \mathbf{k}_2 (\mu_1 k_1 + \mu_2 k_2) / (2k_1^2 k_2^2)$	$-4/\mathcal{H}$
$\delta' \partial_{\parallel} v$	Γ_{11}	$i f^2 \mathcal{H}^2 (\mu_1 k_2 + \mu_2 k_1) / (2k_1 k_2)$	$2b_1/\mathcal{H}$
$\delta \partial_{\parallel} v$	Γ_{11}	$i f \mathcal{H} (\mu_1 k_2 + \mu_2 k_1) / (2k_1 k_2)$	$2b_1(b_e - 2\mathcal{Q} - R) + S$
$\Phi\partial_{\parallel}^3v$	Γ_{12}	$3i f \Omega_m \mathcal{H}^3 (\mu_1^3 k_1^3 + \mu_2^3 k_2^3) / (4k_1^2 k_2^2)$	$-2/\mathcal{H}^2$
$\partial_{\parallel} v \partial_{\parallel}^2 v$	Γ_{13}	$-i f^2 \mathcal{H}^2 (\mu_1 \mu_2^2 k_2 + \mu_2 \mu_1^2 k_1) / (2k_1 k_2)$	$2(3 - 2b_e + 4\mathcal{Q} + 2R + \mathcal{H}'/\mathcal{H}^2)/\mathcal{H}$
$\partial_{\parallel} v \partial_{\parallel}^2 \Phi$	Γ_{13}	$3i f \Omega_m \mathcal{H}^3 (\mu_1 \mu_2^2 k_2 + \mu_2 \mu_1^2 k_1) / (4k_1 k_2)$	$2/\mathcal{H}^2$
$\partial_{\parallel} v^{(2)}$	Γ_{14}	$i f \mathcal{H} \mu_3 G_2(\mathbf{k}_1, \mathbf{k}_2) / k_3$	$b_e - 2\mathcal{Q} - R$

where $\mathcal{A}, \mathcal{B}, \mathcal{C}, \mathcal{D}, \mathcal{E}$ are given by (32)–(36), and

$$R \equiv \frac{2(1-\mathcal{Q})}{\chi\mathcal{H}} + \frac{\mathcal{H}'}{\mathcal{H}^2}, \quad S \equiv 4 \left(2 - \frac{1}{\chi\mathcal{H}} \right) \frac{\partial b_1}{\partial \ln L}. \quad (\text{B11})$$

Note that the kernels for quadratic terms in Table II can be obtained from an algorithm. Consider a term such as

$$\text{D}^n X \text{D}^m Y, \quad (\text{B12})$$

where $\text{D} = \partial_i$ or ∂_{\parallel} , and $X, Y = \delta, v$ or Φ . The corresponding term in the kernel is formed as follows:

$$\begin{aligned} & \left\{ \frac{1}{2} (i k_1)^n (i k_2)^m \text{ for } \text{D} = \partial_{\parallel} \text{ OR } \frac{1}{2} (i \mathbf{k}_1 \cdot i \mathbf{k}_2)^n \text{ for } \text{D} = \partial_i, m = n \right. \\ & \times [k_1^{-2} \text{ if } X \text{ is } v \text{ or } \Phi] \times [k_2^{-2} \text{ if } Y \text{ is } v \text{ or } \Phi] \\ & \times [\text{a factor of } \mu_1 \text{ for each } \partial_{\parallel} \text{ acting on } X] \times [\text{a factor of } \mu_2 \text{ for each } \partial_{\parallel} \text{ acting on } Y] \\ & \times [\text{a factor of } f\mathcal{H} \text{ for each } v] \\ & \times [\text{a factor of } -\frac{3}{2}\Omega_m\mathcal{H}^2 \text{ for each } \Phi] \left. \right\} \\ & + \left\{ 1 \leftrightarrow 2 \right\} \end{aligned} \quad (\text{B13})$$

Appendix C: The coefficients in the GR kernel $\mathcal{K}_{\text{GR}}^{(2)}$

The coefficients $\Gamma_I(z)$ in (55) follow from (30)–(36), using Table II.

Evolution bias b_e and magnification bias \mathcal{Q} make the Γ_I much more complicated than for the case $b_e = 0 = \mathcal{Q}$, which is considered in [28]. (Note that when $\mathcal{Q} = 0$, all the terms with $\partial/\partial \ln \bar{L}$ vanish.)

$$\begin{aligned}
\frac{\Gamma_1}{\mathcal{H}^4} = & \frac{9}{4}\Omega_m^2 \left[-3 + 2f \left(2 - 2b_e + 4\mathcal{Q} + \frac{4(1-\mathcal{Q})}{\chi\mathcal{H}} + \frac{2\mathcal{H}'}{\mathcal{H}^2} \right) - \frac{2f'}{\mathcal{H}} + b_e^2 + 6b_e - 8b_e\mathcal{Q} + 4\mathcal{Q} + 16\mathcal{Q}^2 - 16 \frac{\partial\mathcal{Q}}{\partial \ln \bar{L}} \right. \\
& - 8 \frac{\mathcal{Q}'}{\mathcal{H}} + \frac{b'_e}{\mathcal{H}} + \frac{2}{\chi^2\mathcal{H}^2} \left(1 - \mathcal{Q} + 2\mathcal{Q}^2 - 2 \frac{\partial\mathcal{Q}}{\partial \ln \bar{L}} \right) - \frac{2}{\chi\mathcal{H}} \left(4 + 2b_e - 2b_e\mathcal{Q} - 4\mathcal{Q} + 8\mathcal{Q}^2 - \frac{3\mathcal{H}'}{\mathcal{H}^2} (1 - \mathcal{Q}) \right. \\
& \left. \left. - 8 \frac{\partial\mathcal{Q}}{\partial \ln \bar{L}} - 2 \frac{\mathcal{Q}'}{\mathcal{H}} \right) + \frac{\mathcal{H}'}{\mathcal{H}^2} \left(-8 - 2b_e + 8\mathcal{Q} + \frac{3\mathcal{H}'}{\mathcal{H}^2} \right) - \frac{\mathcal{H}''}{\mathcal{H}^3} \right] \\
& + 3\Omega_m f \left[6 - f(3 - b_e) + b_e \left(3 + \frac{2(1-\mathcal{Q})}{\chi\mathcal{H}} \right) - \frac{b'_e}{\mathcal{H}} - b_e^2 + 4b_e\mathcal{Q} - 12\mathcal{Q} - \frac{6(1-\mathcal{Q})}{\chi\mathcal{H}} + 2 \left(2 - \frac{1}{\chi\mathcal{H}} \right) \frac{\mathcal{Q}'}{\mathcal{H}} \right] \\
& + f^2 \left[12 - 7b_e + b_e^2 + \frac{b'_e}{\mathcal{H}} + (b_e - 3) \frac{\mathcal{H}'}{\mathcal{H}^2} \right] \tag{C1}
\end{aligned}$$

$$\begin{aligned}
\frac{\Gamma_2}{\mathcal{H}^3} = & \frac{9}{4}\Omega_m^2 (f - 2 + 2\mathcal{Q}) + \frac{3}{2}\Omega_m f \left[-2 - f \left(-3 + f + 2b_e - 3\mathcal{Q} - \frac{4(1-\mathcal{Q})}{\chi\mathcal{H}} - \frac{2\mathcal{H}'}{\mathcal{H}^2} \right) - \frac{f'}{\mathcal{H}} + 3b_e + b_e^2 - 6b_e\mathcal{Q} + 4\mathcal{Q} \right. \\
& + 8\mathcal{Q}^2 - 8 \frac{\partial\mathcal{Q}}{\partial \ln \bar{L}} - 6 \frac{\mathcal{Q}'}{\mathcal{H}} + \frac{b'_e}{\mathcal{H}} + \frac{2}{\chi^2\mathcal{H}^2} \left(1 - \mathcal{Q} + 2\mathcal{Q}^2 - 2 \frac{\partial\mathcal{Q}}{\partial \ln \bar{L}} \right) + \frac{2}{\chi\mathcal{H}} \left(-1 - 2b_e + 2b_e\mathcal{Q} + \mathcal{Q} - 6\mathcal{Q}^2 \right. \\
& + \frac{3\mathcal{H}'}{\mathcal{H}^2} (1 - \mathcal{Q}) + 6 \frac{\partial\mathcal{Q}}{\partial \ln \bar{L}} + 2 \frac{\mathcal{Q}'}{\mathcal{H}} \left. \right) - \frac{\mathcal{H}'}{\mathcal{H}^2} \left(3 + 2b_e - 6\mathcal{Q} - \frac{3\mathcal{H}'}{\mathcal{H}^2} \right) - \frac{\mathcal{H}''}{\mathcal{H}^3} \left. \right] + f^2 \left[-3 + 2b_e \left(2 + \frac{(1-\mathcal{Q})}{\chi\mathcal{H}} \right) \right. \\
& \left. - b_e^2 + 2b_e\mathcal{Q} - 6\mathcal{Q} - \frac{b'_e}{\mathcal{H}} - \frac{6(1-\mathcal{Q})}{\chi\mathcal{H}} + 2 \left(1 - \frac{1}{\chi\mathcal{H}} \right) \frac{\mathcal{Q}'}{\mathcal{H}} \right] \tag{C2}
\end{aligned}$$

$$\frac{\Gamma_3}{\mathcal{H}^2} = \frac{3}{2}\Omega_m \left[2 - 2f + b_e - 4\mathcal{Q} - \frac{2(1-\mathcal{Q})}{\chi\mathcal{H}} - \frac{\mathcal{H}'}{\mathcal{H}^2} \right] \tag{C3}$$

$$\frac{\Gamma_4}{\mathcal{H}^2} = f(3 - b_e) \tag{C4}$$

$$\begin{aligned}
\frac{\Gamma_5}{\mathcal{H}^2} = & 3\Omega_m f (2 - f - 2\mathcal{Q}) + f^2 \left[4 + b_e - b_e^2 + 4b_e\mathcal{Q} - 6\mathcal{Q} - 4\mathcal{Q}^2 + 4 \frac{\partial\mathcal{Q}}{\partial \ln \bar{L}} + 4 \frac{\mathcal{Q}'}{\mathcal{H}} - \frac{b'_e}{\mathcal{H}} \right. \\
& - \frac{2}{\chi^2\mathcal{H}^2} \left(1 - \mathcal{Q} + 2\mathcal{Q}^2 - 2 \frac{\partial\mathcal{Q}}{\partial \ln \bar{L}} \right) - \frac{2}{\chi\mathcal{H}} \left(3 - 2b_e + 2b_e\mathcal{Q} - \mathcal{Q} - 4\mathcal{Q}^2 + \frac{3\mathcal{H}'}{\mathcal{H}^2} (1 - \mathcal{Q}) + 4 \frac{\partial\mathcal{Q}}{\partial \ln \bar{L}} + 2 \frac{\mathcal{Q}'}{\mathcal{H}} \right) \\
& \left. - \frac{\mathcal{H}'}{\mathcal{H}^2} \left(3 - 2b_e + 4\mathcal{Q} + \frac{3\mathcal{H}'}{\mathcal{H}^2} \right) + \frac{\mathcal{H}''}{\mathcal{H}^3} \right] \tag{C5}
\end{aligned}$$

$$\frac{\Gamma_6}{\mathcal{H}^2} = 3\Omega_m f - f^2 \left[-1 + b_e - 2\mathcal{Q} - \frac{2(1+\mathcal{Q})}{\chi\mathcal{H}} - \frac{\mathcal{H}'}{\mathcal{H}^2} \right] \tag{C6}$$

$$\frac{\Gamma_7}{\mathcal{H}^2} = \frac{3}{2}\Omega_m \left[b_1 \left(2 + b_e - 4\mathcal{Q} - \frac{2(1-\mathcal{Q})}{\chi\mathcal{H}} - \frac{\mathcal{H}'}{\mathcal{H}^2} \right) + \frac{b'_1}{\mathcal{H}} + 2 \left(2 - \frac{1}{\chi\mathcal{H}} \right) \frac{\partial b_1}{\partial \ln \bar{L}} \right] - f \left[b_1 (f - 3 + b_e) + \frac{b'_1}{\mathcal{H}} \right] \tag{C7}$$

$$\frac{\Gamma_8}{\mathcal{H}^2} = \frac{9}{4}\Omega_m^2 + \frac{3}{2}\Omega_m f \left[1 - 2f + 2b_e - 6\mathcal{Q} - \frac{4(1-\mathcal{Q})}{\chi\mathcal{H}} - \frac{3\mathcal{H}'}{\mathcal{H}^2} \right] + f^2 (3 - b_e) \tag{C8}$$

$$\frac{\Gamma_9}{\mathcal{H}} = -\frac{3}{2}\Omega_m b_1 \quad (\text{C9})$$

$$\frac{\Gamma_{10}}{\mathcal{H}} = 2f^2 \quad (\text{C10})$$

$$\frac{\Gamma_{11}}{\mathcal{H}} = f \left[b_1 \left(f + b_e - 2\mathcal{Q} - \frac{2(1-\mathcal{Q})}{\chi\mathcal{H}} - \frac{\mathcal{H}'}{\mathcal{H}^2} \right) + \frac{b_1'}{\mathcal{H}} + 2 \left(1 - \frac{1}{\chi\mathcal{H}} \right) \frac{\partial b_1}{\partial \ln \bar{L}} \right] \quad (\text{C11})$$

$$\frac{\Gamma_{12}}{\mathcal{H}} = -\frac{3}{2}\Omega_m f \quad (\text{C12})$$

$$\frac{\Gamma_{13}}{\mathcal{H}} = \frac{3}{2}\Omega_m f - f^2 \left[3 - 2b_e + 4\mathcal{Q} + \frac{4(1-\mathcal{Q})}{\chi\mathcal{H}} + \frac{3\mathcal{H}'}{\mathcal{H}^2} \right] \quad (\text{C13})$$

$$\frac{\Gamma_{14}}{\mathcal{H}} = f \left[b_e - 2\mathcal{Q} - \frac{2(1-\mathcal{Q})}{\chi\mathcal{H}} - \frac{\mathcal{H}'}{\mathcal{H}^2} \right] \quad (\text{C14})$$

-
- [1] J. C. Jackson, *Fingers of God: A critique of Rees' theory of primordial gravitational radiation*, *Mon. Not. Roy. Astron. Soc.* **156** (1972) 1P–5P, [arXiv:0810.3908].
- [2] W. L. W. Sargent and E. L. Turner, *A statistical method for determining the cosmological density parameter from the redshifts of a complete sample of galaxies*, *Astrophys. J.* **212** (Feb., 1977) L3–L7.
- [3] N. Kaiser, *Clustering in real space and in redshift space*, *Mon. Not. Roy. Astron. Soc.* **227** (1987) 1–27.
- [4] R. Moessner and B. Jain, *Angular cross-correlation of galaxies: a probe of gravitational lensing by large scale structure*, *Mon. Not. Roy. Astron. Soc.* **294** (1998) 18, [astro-ph/9709159].
- [5] L. Hui, E. Gaztanaga, and M. LoVerde, *Anisotropic Magnification Distortion of the 3D Galaxy Correlation. 1. Real Space*, *Phys. Rev.* **D76** (2007) 103502, [arXiv:0706.1071].
- [6] L. Hui, E. Gaztanaga, and M. LoVerde, *Anisotropic Magnification Distortion of the 3D Galaxy Correlation: II. Fourier and Redshift Space*, *Phys. Rev.* **D77** (2008) 063526, [arXiv:0710.4191].
- [7] D. Alonso, P. Bull, P. G. Ferreira, R. Maartens, and M. G. Santos, *Ultra-large scale cosmology with next-generation experiments*, *Astrophys. J.* **814** (2015) 145, [arXiv:1505.07596].
- [8] F. Montanari and R. Durrer, *Measuring the lensing potential with tomographic galaxy number counts*, *JCAP* **1510** (2015), no. 10 070, [arXiv:1506.01369].
- [9] A. M. Dizgah and R. Durrer, *Lensing corrections to the $E_g(z)$ statistics from large scale structure*, *JCAP* **1609** (2016) 035, [arXiv:1604.08914].
- [10] J. Yoo, *General Relativistic Description of the Observed Galaxy Power Spectrum: Do We Understand What We Measure?*, *Phys. Rev.* **D82** (2010) 083508, [arXiv:1009.3021].
- [11] A. Challinor and A. Lewis, *The linear power spectrum of observed source number counts*, *Phys. Rev.* **D84** (2011) 043516, [arXiv:1105.5292].
- [12] C. Bonvin and R. Durrer, *What galaxy surveys really measure*, *Phys. Rev.* **D84** (2011) 063505, [arXiv:1105.5280].
- [13] M. Bruni, R. Crittenden, K. Koyama, R. Maartens, C. Pitrou, and D. Wands, *Disentangling non-Gaussianity, bias and GR effects in the galaxy distribution*, *Phys. Rev.* **D85** (2012) 041301, [arXiv:1106.3999].
- [14] T. Baldauf, U. Seljak, L. Senatore, and M. Zaldarriaga, *Galaxy Bias and non-Linear Structure Formation in General Relativity*, *JCAP* **1110** (2011) 031, [arXiv:1106.5507].
- [15] D. Jeong, F. Schmidt, and C. M. Hirata, *Large-scale clustering of galaxies in general relativity*, *Phys. Rev.* **D85** (2012) 023504, [arXiv:1107.5427].
- [16] S. Camera, M. G. Santos, and R. Maartens, *Probing primordial non-Gaussianity with SKA galaxy redshift surveys: a fully relativistic analysis*, *Mon. Not. Roy. Astron. Soc.* **448** (2015), no. 2 1035–1043, [arXiv:1409.8286].
- [17] S. Camera, R. Maartens, and M. G. Santos, *Einstein's legacy in galaxy surveys*, *Mon. Not. Roy. Astron. Soc.* **451** (2015), no. 1 L80–L84, [arXiv:1412.4781].
- [18] E. Sefusatti, M. Crocce, S. Pueblas, and R. Scoccimarro, *Cosmology and the Bispectrum*, *Phys. Rev.* **D74** (2006) 023522, [astro-ph/0604505].
- [19] E. Sefusatti and E. Komatsu, *The bispectrum of galaxies from high-redshift galaxy surveys: Primordial non-Gaussianity and non-linear galaxy bias*, *Phys. Rev.* **D76** (2007) 083004, [arXiv:0705.0343].
- [20] L. Verde, A. F. Heavens, S. Matarrese, and L. Moscardini, *Large scale bias in the universe. 2. Redshift space bispectrum*, *Mon. Not. Roy. Astron. Soc.* **300** (1998) 747–756, [astro-ph/9806028].
- [21] R. Scoccimarro, H. Couchman, and J. A. Frieman, *The Bispectrum as a signature of gravitational instability in redshift-space*, *Astrophys. J.* **517** (1999) 531–540, [astro-ph/9808305].
- [22] F. Schmidt, A. Vallinotto, E. Sefusatti, and S. Dodelson, *Weak Lensing Effects on the Galaxy Three-Point Correlation Function*, *Phys. Rev.* **D78** (2008) 043513, [arXiv:0804.0373].
- [23] H. Gil-Marín, W. J. Percival, L. Verde, J. R. Brownstein, C.-H. Chuang, F.-S. Kitaura, S. A. Rodríguez-Torres, and M. D. Olmstead, *The clustering of galaxies in the SDSS-III Baryon Oscillation Spectroscopic Survey: RSD measurement from the power spectrum and bispectrum of the DR12 BOSS galaxies*, *Mon. Not. Roy. Astron. Soc.* **465** (2017), no. 2 1757–1788, [arXiv:1606.00439].
- [24] Z. Slepian et al., *Detection of Baryon Acoustic Oscillation Features in the Large-Scale 3-Point Correlation Function of SDSS BOSS DR12 CMASS Galaxies*, arXiv:1607.06097.
- [25] M. Tellarini, A. J. Ross, G. Tasinato, and D. Wands, *Galaxy bispectrum, primordial non-Gaussianity and redshift space distortions*, *JCAP* **1606** (2016), no. 06 014, [arXiv:1603.06814].
- [26] E. Di Dio, R. Durrer, G. Marozzi, and F. Montanari, *The bispectrum of relativistic galaxy number counts*, *JCAP* **1601** (2016) 016, [arXiv:1510.04202].
- [27] A. Kehagias, A. M. Dizgah, J. Norea, H. Perrier, and A. Riotto, *A Consistency Relation for the Observed Galaxy Bispectrum and the Local non-Gaussianity from Relativistic Corrections*, *JCAP* **1508** (2015), no. 08 018, [arXiv:1503.04467].
- [28] O. Umeh, S. Jolicoeur, R. Maartens, and C. Clarkson, *A general relativistic signature in the galaxy bispectrum: the local effects of observing on the lightcone*, *JCAP* **1703** (2017) 003, [arXiv:1610.03351].
- [29] D. Bertacca, *Observed galaxy number counts on the light cone up to second order: III. Magnification bias*, *Class. Quant. Grav.* **32** (2015), no. 19 195011, [arXiv:1409.2024].
- [30] D. Bertacca, R. Maartens, and C. Clarkson, *Observed galaxy number counts on the lightcone up to second order: I. Main result*, *JCAP* **1409** (2014), no. 09 037, [arXiv:1405.4403].

- [31] D. Bertacca, R. Maartens, and C. Clarkson, *Observed galaxy number counts on the lightcone up to second order: II. Derivation*, *JCAP* **1411** (2014), no. 11 013, [[arXiv:1406.0319](#)].
- [32] J. Yoo and M. Zaldarriaga, *Beyond the Linear-Order Relativistic Effect in Galaxy Clustering: Second-Order Gauge-Invariant Formalism*, *Phys. Rev.* **D90** (2014), no. 2 023513, [[arXiv:1406.4140](#)].
- [33] E. Di Dio, R. Durrer, G. Marozzi, and F. Montanari, *Galaxy number counts to second order and their bispectrum*, *JCAP* **1412** (2014) 017, [[arXiv:1407.0376](#)]. [Erratum: *JCAP*1506,no.06,E01(2015)].
- [34] E. Di Dio, H. Perrier, R. Durrer, G. Marozzi, A. M. Dizgah, J. Norea, and A. Riotto, *Non-Gaussianities due to Relativistic Corrections to the Observed Galaxy Bispectrum*, *JCAP* **1703** (2017), no. 03 006, [[arXiv:1611.03720](#)].
- [35] T. Tram, C. Fidler, R. Crittenden, K. Koyama, G. W. Pettinari, and D. Wands, *The Intrinsic Matter Bispectrum in Λ CDM*, *JCAP* **1605** (2016), no. 05 058, [[arXiv:1602.05933](#)].
- [36] S. Mollerach and S. Matarrese, *Cosmic microwave background anisotropies from second order gravitational perturbations*, *Phys. Rev.* **D56** (1997) 4494–4502, [[astro-ph/9702234](#)].
- [37] S. Matarrese, S. Mollerach, and M. Bruni, *Second order perturbations of the Einstein-de Sitter universe*, *Phys. Rev.* **D58** (1998) 043504, [[astro-ph/9707278](#)].
- [38] T. H.-C. Lu, K. Ananda, C. Clarkson, and R. Maartens, *The cosmological background of vector modes*, *JCAP* **0902** (2009) 023, [[arXiv:0812.1349](#)].
- [39] M. Bruni, D. B. Thomas, and D. Wands, *Computing General Relativistic effects from Newtonian N-body simulations: Frame dragging in the post-Friedmann approach*, *Phys. Rev.* **D89** (2014), no. 4 044010, [[arXiv:1306.1562](#)].
- [40] K. N. Ananda, C. Clarkson, and D. Wands, *The Cosmological gravitational wave background from primordial density perturbations*, *Phys. Rev.* **D75** (2007) 123518, [[gr-qc/0612013](#)].
- [41] D. Baumann, P. J. Steinhardt, K. Takahashi, and K. Ichiki, *Gravitational Wave Spectrum Induced by Primordial Scalar Perturbations*, *Phys. Rev.* **D76** (2007) 084019, [[hep-th/0703290](#)].
- [42] D. Jeong and F. Schmidt, *Large-Scale Structure with Gravitational Waves I: Galaxy Clustering*, *Phys. Rev.* **D86** (2012) 083512, [[arXiv:1205.1512](#)].
- [43] **Planck** Collaboration, P. A. R. Ade et al., *Planck 2015 results. XIII. Cosmological parameters*, *Astron. Astrophys.* **594** (2016) A13, [[arXiv:1502.01589](#)].
- [44] C. Bonvin, *Effect of Peculiar Motion in Weak Lensing*, *Phys. Rev.* **D78** (2008) 123530, [[arXiv:0810.0180](#)].
- [45] D. Bertacca, N. Bartolo, M. Bruni, K. Koyama, R. Maartens, S. Matarrese, M. Sasaki, and D. Wands, *Galaxy bias and gauges at second order in General Relativity*, *Class. Quant. Grav.* **32** (2015), no. 17 175019, [[arXiv:1501.03163](#)].
- [46] E. Villa and C. Rampf, *Relativistic perturbations in Λ CDM: Eulerian & Lagrangian approaches*, *JCAP* **1601** (2016), no. 01 030, [[arXiv:1505.04782](#)].
- [47] D. Bertacca, *Private communication (Erratum for [29] to appear)*, .
- [48] L. Dai, E. Pajer, and F. Schmidt, *On Separate Universes*, *JCAP* **1510** (2015), no. 10 059, [[arXiv:1504.00351](#)].
- [49] R. de Putter, O. Doré, and D. Green, *Is There Scale-Dependent Bias in Single-Field Inflation?*, *JCAP* **1510** (2015), no. 10 024, [[arXiv:1504.05935](#)].
- [50] N. Bartolo, D. Bertacca, M. Bruni, K. Koyama, R. Maartens, S. Matarrese, M. Sasaki, L. Verde, and D. Wands, *A relativistic signature in large-scale structure*, *Phys. Dark Univ.* **13** (2016) 30–34, [[arXiv:1506.00915](#)].
- [51] F. Bernardeau, S. Colombi, E. Gaztanaga, and R. Scoccimarro, *Large scale structure of the universe and cosmological perturbation theory*, *Phys. Rept.* **367** (2002) 1–248, [[astro-ph/0112551](#)].
- [52] P. Gagrani and L. Samushia, *Information Content of the Angular Multipoles of Redshift-Space Galaxy Bispectrum*, [arXiv:1610.03488](#).
- [53] J. E. Pollack, R. E. Smith, and C. Porciani, *A new method to measure galaxy bias*, *Mon. Not. Roy. Astron. Soc.* **440** (2014) 555, [[arXiv:1309.0504](#)].
- [54] D. Bertacca, A. Raccanelli, N. Bartolo, M. Liguori, S. Matarrese, and L. Verde, *Relativistic wide-angle galaxy bispectrum on the light-cone*, [arXiv:1705.09306](#).